LIMNOLOGY
and
OCEANOGRAPHY

ASLO

Limnol. Oceanogr. 63, 2018, 47–71

doi: 10.1002/lno.10614

Inorganic carbon and oxygen dynamics in a marsh-dominated estuary

Shiyu Rachel Wang ,[1]* **Daniela Di Iorio,**[1] **Wei-Jun Cai,**[2] **Charles S. Hopkinson**[1]
[1]Department of Marine Sciences, The University of Georgia, Athens, Georgia
[2]School of Marine Science and Policy, The University of Delaware, Newark, Delaware

Abstract

We conducted a free-water mass balance-based study to address the rate of metabolism and net carbon exchange for the tidal wetland and estuarine portion of the coastal ocean and the uncertainties associated with this approach were assessed. We measured open water diurnal O_2 and dissolved inorganic carbon (DIC) dynamics seasonally in a salt marsh-estuary in Georgia, U.S.A. with a focus on the marsh-estuary linkage associated with tidal flooding. We observed that the overall estuarine system was a net source of CO_2 to the atmosphere and coastal ocean and a net sink for oceanic and atmospheric O_2. Rates of metabolism were extremely high, with respiration (43 mol m^{-2} yr^{-1}) greatly exceeding gross primary production (28 mol m^{-2} yr^{-1}), such that the overall system was net heterotrophic. Metabolism measured with DIC were higher than with O_2, which we attribute to high rates of anaerobic respiration and reduced sulfur storage in salt marsh sediments, and we assume substantial levels of anoxygenic photosynthesis. We found gas exchange from a flooded marsh is substantial, accounting for about 28% of total O_2 and CO_2 air–water exchange. A significant percentage of the overall estuarine aquatic metabolism is attributable to metabolism of marsh organisms during inundation. Our study suggests not rely on oceanographic stoichiometry to convert from O_2 to C based measurements when constructing C balances for the coastal ocean. We also suggest eddy covariance measurements of salt marsh net ecosystem exchange underestimate net ecosystem production as they do not account for lateral DIC exchange associated with marsh tidal inundation.

Carbon dynamics of salt marsh-dominated estuaries have fascinated coastal ecosystem ecologists for more than half a century because of their tremendously high rates of primary production, their support for commercial fisheries, and their disproportionately large contribution to the global carbon budget relative to their size (Bauer et al. 2013). Early investigations documented their high rates of marsh primary production and little apparent grazing and organic matter burial. Large quantities of macrophyte-derived organic matter were exported to tidal waters where it formed the basis of a rich detrital food web (Teal 1962; Darnell 1967; Odum 1968). Aquatic and benthic metabolism measurements of estuarine subsystems in bottles and chambers supported a marsh outwelling hypothesis by showing a deficit of production relative to respiration (e.g., Hopkinson 1985; Cai et al. 1999), but cross-system comparisons of coastal fisheries production found little evidence that it was higher in salt marsh-dominated estuaries (Nixon 1980). Carbon budgets became increasingly complex through the 1980s following decades of observations, but many fluxes, including those between marsh and tidal creeks, were calculated by mass balance (Hopkinson 1988) and oftentimes the uncertainties were quite large. More recently, mass balance analysis of CO_2 degassing from estuarine waters and dissolved inorganic carbon (DIC) export from salt marsh-dominated estuaries suggests large export of inorganic carbon from salt marsh-estuaries but how much of this carbon originates as respiration on the marsh proper as opposed to respiration in tidal creeks of organic matter exported from the marsh is not entirely clear (Wang and Cai 2004; Cai 2011). Recent global syntheses of the coastal ocean carbon balance conclude that tremendous spatial heterogeneity in carbon processing and fluxes results in high levels of uncertainty in estuarine net carbon balances and that climate change, land-use change, and sea-level rise will likely decrease net carbon burial in estuaries and adjacent tidal wetlands in the future (Bauer et al. 2013).

We suggest that further progress in refining marsh-estuarine carbon fluxes and reducing uncertainty in metabolic balance will be made by reducing three major

*Correspondence: sywang@uga.edu

Additional Supporting Information may be found in the online version of this article.

constraints: (1) chamber and bottle approaches to measuring metabolism of marsh-estuarine subsystems (e.g., intertidal benthos and marsh platform) likely severely underestimate true rates, as they artificially separate local sources and sinks of nutrients, reduce mixing, reduce macrofaunal feedbacks and lack the tidal dynamics of intertidal flat and marsh platform flooding and draining (Montague 1980; Smith and Hollibaugh 1997), (2) scaling plot-based measures (e.g., subtidal benthos, water column, creekbank) to the whole system typically misrepresents the high spatial heterogeneity of salt marsh estuaries (Cai 2011; Bauer et al. 2013), and (3) calculating whole system net carbon balance from many independent measures of production and respiration, each of which has a high uncertainty, typically results in a small value for net ecosystem metabolism with high variance and even higher uncertainty (Hopkinson 1988).

One way to overcome the constraints of containerization, component isolation and high variance is to directly conduct whole system measures of metabolism including net ecosystem production (NEP), using eddy covariance approaches to measure marsh metabolism (Forbrich and Giblin 2015) and open water diurnal approaches to measure estuarine metabolism (Odum 1956; Swaney et al. 1999; Balsis et al. 1995). With the open water diurnal approach, the metabolism of the multi-component, coupled marsh-estuary system is calculated from the diurnal changes in DIC and/or O_2 after correcting for atmospheric exchange and mixing with adjacent water masses. The free water diurnal approach, apart from providing direct measures of whole system metabolism without constraint, also yields measures of estuarine O_2 and CO_2 exchange with the atmosphere and exchange with coastal ocean waters, which are of great importance in understanding the global atmospheric CO_2 budget and the exchange of carbon between terrestrial and oceanic realms (Cai and Wang 1998; Frankignoulle et al. 1998; Raymond et al. 2000; Cai 2011; Bauer et al. 2013).

In the ocean, known C : N : S : P : O stoichiometry of metabolism suggests that O_2 and CO_2 can be used interchangeably to measure metabolism (Redfield 1958). Indeed, stoichiometrically linked whole-system budgets of C, N, and P have been used to directly measure NEP of coastal systems (sensu Smith and Hollibaugh 1997). Most often however CO_2 and O_2 are used to measure metabolism in isolated containers, but usually separately—$^{14}CO_2$ to measure production because of its sensitivity and O_2 to measure respiration because of its simplicity. With recent interest in understanding the role of various aquatic ecosystems in controlling atmospheric CO_2 levels, prior metabolism studies based on O_2 are being used to calculate CO_2 dynamics. Frequently respiratory and photosynthesis quotients (RQ and PQ) of 1 are used to convert from O_2 to CO_2 (Boynton and Kemp 1985; Hopkinson 1987; Banta et al. 1995), but evidence suggests great caution is required in making this assumption. In shallow water systems, a large percentage of metabolism is benthic and dependent on alternative electron acceptors to O_2, such as NO_3^-, oxidized forms of Fe and Mn, and SO_4^{2-}. Respiration in salt marsh and estuarine sediments is dominated by SO_4^{2-} reduction, thus decoupling of O_2 and CO_2 at least temporally. The decoupling of O_2 and CO_2 can also be a result of differences in thermodynamic and gas exchange dynamic controls of the O_2 and CO_2 gases as CO_2 is buffered by a vast marine HCO_3^- system while O_2 is the sole molecule. It is essential that we understand the temporal and spatial variability in the stoichiometry of O_2 and CO_2 if we continue to use O_2 to measure coastal metabolism for use in global C budgets.

In one of the first inorganic carbon balance studies of salt marsh estuaries, Wang and Cai (2004) found that inorganic carbon was exported at high rates from estuarine waters, both in terms of CO_2 flux to the atmosphere and DIC transport to the coastal ocean. In comparison to bottle measures of estuarine aquatic respiration, Wang and Cai concluded that an important source of the exported DIC was the salt marsh. Previous organic carbon budgets had ignored inorganic carbon and concluded that the super-saturation of estuarine waters with CO_2 and under-saturation with O_2 was the sole result of the decomposition of organic carbon exported from the marsh. The open water diurnal approach to salt marsh estuarine metabolism directly incorporates some contribution of salt marsh metabolism to adjacent tidal waters, as twice daily high tides flood the marsh platform resulting in either the uptake or release of DIC and oxygen as results of metabolism on the marsh.

In this study, we used the open water diurnal approach to study the seasonal metabolism of a hydrodynamically linked salt marsh-estuary, the Duplin River in Georgia, U.S.A. We used simultaneous measurements of DIC, the partial pressure of CO_2 (pCO_2) and O_2 along the entire 12 km length of this system to examine the stoichiometry of CO_2 and O_2 and to integrate across a highly heterogeneous complex of open water, intertidal flats, marsh creekbanks, tidal creeks, and marsh platform environments. We also measured directly the flux of DIC and O_2 between the Duplin River and an adjacent first-order tidal creek and its watershed in order to evaluate the contribution of marsh flooding to the metabolism of the Duplin River. In addition, we measured the air to water and marsh-estuary to coastal ocean exchange of DIC, CO_2, and O_2. This work was done in parallel with eddy covariance measures of net ecosystem exchange (NEE) of CO_2 between a Duplin River marsh and the atmosphere.

Study site and methods

Study site

We conducted our study in the Duplin River salt marsh-estuary, adjacent to Sapelo Island, Georgia, a coastal ecosystem representative of the broad intertidal, wetland macrophyte-dominated estuaries of the Carolinean biogeographic province of the southeastern U.S.A (Fig. 1). The ecosystem is relatively pristine as local coastal development is low.

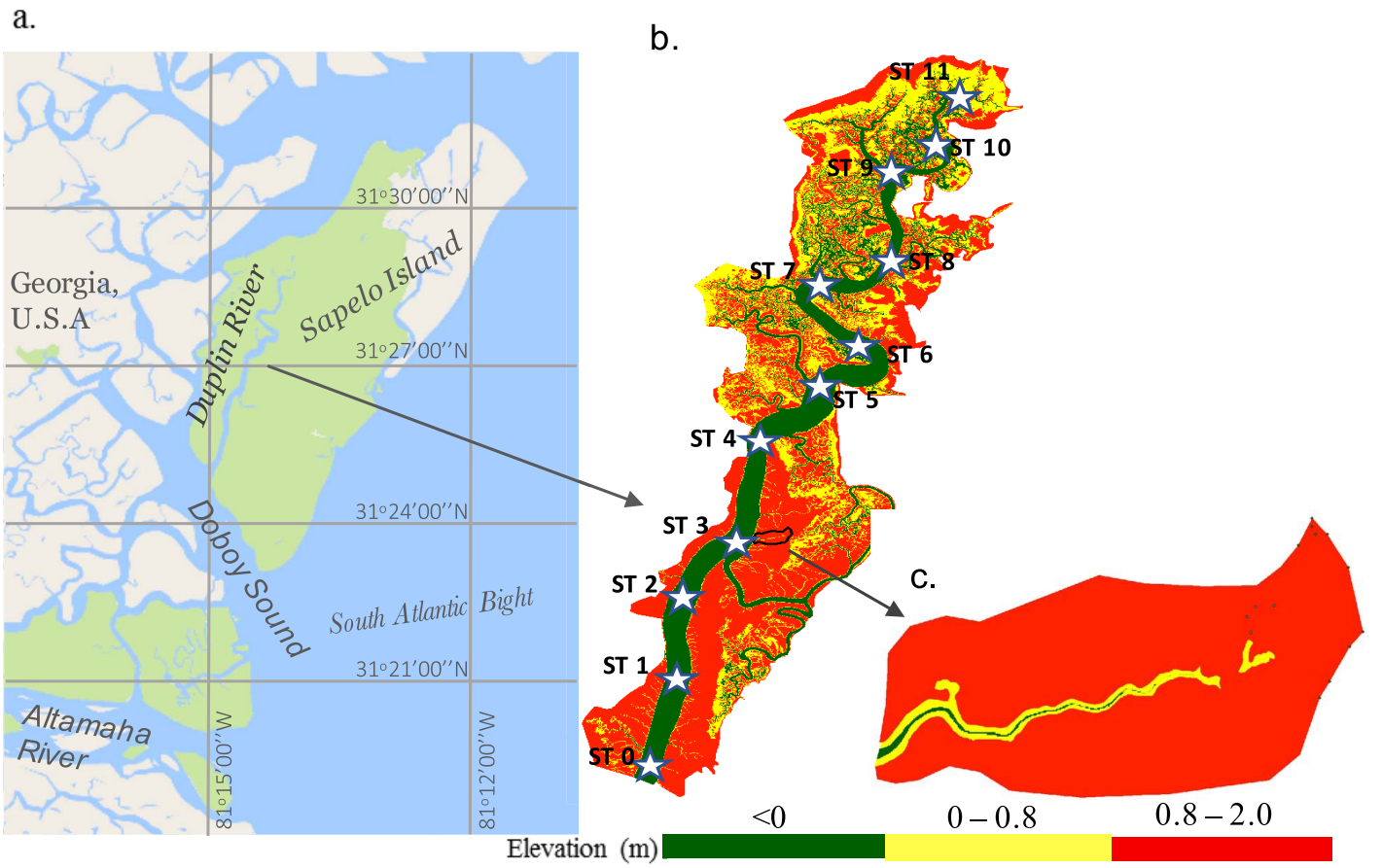

Fig. 1. Study site and sampling stations. (**a**) Sapelo Island and its relative location, (**b**) the Duplin River and its salt marsh catchment: shown are the locations of our 12 equally spaced, low-tide sampling stations (STs 0–11 white stars on green river). Sta. 0 has coordinates 31°25.090′ N by 81°17.810′ W. (**c**) Flux tower tidal creek and its marsh catchment: Dots to the far right show where GPS sampling confirmed catchment boundaries. Dots near the head of the creek show the end of the boardwalk that accesses the eddy covariance flux tower. The color scheme shows three regions delineated by elevation: (1) permanently open water, benthos, and intertidal mud flats (dark green): < 0 m MSL, (2) rapidly sloping creekbanks with tall *S. alterniflora*, whose pore water drains extensively at low tide (yellow: 0–0.8 m and 3) the wide, extensive high marsh platform, which typically has stunted *S. alterniflora* (red): 0.8–2 m MSL. Elevations are converted from NAVD88 such that 0 m elevation corresponds to MSL as determined relative to NOAA benchmarks near our site.

The Duplin salt marsh-estuary ecosystem includes the Duplin River estuary and the adjacent intertidal salt marsh that floods at high tide (consider the intertidal marshes as the catchment or watershed for the Duplin River). The ecosystem is approximately 12-km long and 11.4 km^2 in area of which about 30% is aquatic (20% permanently aquatic with depths below mean low water [MLW]: −1.02 m relative to mean sea level [MSL]: 0 m and 10% intertidal mudflats between MLW and MSL) and 70% is intertidal salt marsh. The marsh, which is dominated by *Spartina alterniflora*, extends from near 0 m MSL to form a broad relatively flat platform between about 0.8 to about 1.2 m in elevation. Mean high water is at 1.0 m.

The meso-tidal Duplin River is well-mixed (Type 1B by the Hansen and Rattray (1966) classification criteria) with minimal freshwater input that is mostly via groundwater runoff from Sapelo Island and freshwater that comes in at the mouth during high Altamaha River discharge periods (Imberger et al. 1983). Salinity varies seasonally in relation to discharge of the Altamaha River about 10 km to the south (Fig. 1). The Duplin has a large tidal excursion that decreases along its length from about 3.9 km at the mouth to about 1 km at its upper end (Ragotzkie and Bryson 1955; Imberger et al. 1983; this study). We identified two water masses within the Duplin River based on whether the water mass remains in the system at low tide or exchanges with Doboy Sound and the coastal ocean. Our study was conducted in the "resident" water mass that remains within the Duplin at low tide.

Our study measured the inorganic C and O_2 dynamics including the air–water exchange, the longitudinal mixing, and the calculated metabolism in the "resident" water, which remains in the channel of the estuary during low tide, in the 12-km long Duplin River. We also measured the

metabolism and inorganic C and O_2 dynamics of water when it floods the marsh by focusing on a first order tidal creek that is the main source of water that floods the marsh and where the Georgia Coastal Ecosystem-Long Term Ecosystem Research (GCE-LTER) project operates an eddy covariance tower. The small tidal creek connects directly with the Duplin River about three kilometers from its mouth (Fig. 1). The small tidal creek is about 400 m long and floods a marsh of 0.043 km^2. It drains completely at low tide, with only a trickle of water flowing during lowest stages of the tide as a result of creek-bank drainage.

Open-water diurnal approach

We investigated carbon dynamics and ecosystem metabolism of "resident water" of the Duplin River salt marsh-estuary seasonally by analyzing the open water (Odum and Hoskin 1958; Odum and Wilson 1962; Balsis et al. 1995) diurnal changes in DIC and dissolved oxygen (DO) along the entire length of the system. We also examined the contribution of intertidal marshes to carbon and oxygen dynamics of the salt marsh-estuary by analyzing the net transport of DIC and O_2 through a small, ephemeral tidal creek that floods a defined salt marsh catchment adjacent to the main Duplin River channel.

Three processes contribute to the diurnal change in DIC and DO concentrations: gas exchange across the air–water surface, longitudinal dispersion or mixing with adjacent water masses and metabolism by the pelagic, benthic, and intertidal communities of the salt marsh-estuary ecosystem when inundated (Eq. 1):

$$\Delta[\mathrm{DIC\ (DO)}] * V = F * A_S * T + M * A_C * T + \mathrm{Metabolism} \quad (1)$$

where Δ[DIC (DO)] is the diurnal change in DIC or DO concentration (mol $m^{-3)}$; V is the water volume (m^3); F is vertical gas flux across air–water surface (mol m^{-2} h^{-1}); A_S is the water surface area (m^2); M is longitudinal mixing flux with adjacent water masses (mol m^{-2} h^{-1}); A_c is cross section area (m^2) of the water channel, T is the time interval (h) for a diurnal cycle.

Water of the Duplin is our reference for Eq. 1 such that positive values for terms increase the concentration of DIC or O_2. For example, a calculated air–water flux of CO_2 of -10 mol m^{-2} d^{-1} would lead to a decrease in DIC for a water mass during a diurnal period.

Spatial sampling along the Duplin

Discrete samples for DIC and total alkalinity (Alk) were collected at twelve 1 km equidistantly spaced stations (Fig. 1), while DO concentration, DO percent saturation (DO %), and pCO_2 were continuously measured along the length of the Duplin. Each transect was run within about 1 h of dawn, dusk and the next dawn on 21–22 February 2014, 19–20 May 2014, 15–16 August 2014, and 29–30 October 2014. Sampling days were chosen so that sunrise was within 2 h of low tide to facilitate matching of dawn-dusk and dusk-dawn sampling station water masses (further details in Supporting Information Appendix A). Synoptic transects typically took 1 h to complete. Details of DIC and Alk sampling, storage and analysis and pCO_2 measurements are described fully in Wang and Cai (2004). DO and its percent saturation were continuously measured with a YSI-6920 along with ancillary data such as temperature, salinity, and chlorophyll fluorescence by pumping water while underway from below the boat hull (Vallino et al. 2005). The YSI was calibrated in moist air at sea level just prior to sampling. Salinity was calibrated against KCl standards. Additional discrete samples were collected for dissolved organic carbon (DOC) as an ancillary parameter to help in explaining the spatial and temporal variability of metabolism along the Duplin. DOC samples were filtered through precombusted Whatman GF/F filters (nominal ~0.7 μm pore size), stored frozen and analyzed on a Shimadzu TOC-Vcph analyzer, paying careful attention to blank correction. Wind velocity and photosynthetically active radiation (PAR) were obtained from continuous measurements made and archived by the GCE-LTER program for a site adjacent to our Sta. 0 near the mouth of the Duplin (Fig. 1).

Air–water exchange

CO_2 and O_2 air–water fluxes (F in Eq. 1) were estimated with the one-dimensional bulk flux equation:

$$F_{CO_2} = K_H * K_T * (pCO_{2water} - pCO_{2atm}) \quad (2)$$

$$F_{O_2} = K_T * (DO_{water} - DO_{atm}) \quad (3)$$

where K_H (mol m^{-3} atm^{-1}) is the CO_2 solubility coefficient calculated as a function of water temperature and salinity (Weiss 1974) ranging from 26.5 mol m^{-3} atm^{-1} to 45.8 mol m^{-3} atm^{-1}; K_T (cm h^{-1}) is gas transfer velocity as a function of wind speed at 10 m above the water surface (Wanninkhof et al. 2009, Eq. 36) ranging from 2.5 cm h^{-1} to 7.0 cm h^{-1}; pCO_2water and pCO_{2atm} are the partial pressure of CO_2 (ppm) of Duplin water and the atmosphere measured underway. DO_{water} is the dissolved oxygen concentration (mol L^{-1}) measured in water. DO_{atm} is the saturated dissolved oxygen concentration calculated from the percent saturation measured with the YSI and takes into consideration temperature and salinity. While the Wanninkhof et al. equation was developed for the open ocean, it met our criteria of agreeing with observations at low wind speeds in a similar wetland-dominated estuary (Parker River estuary, Massachusetts, U.S.A.—Carini et al. 1996 based on SF_6, Zappa et al. 2007 based on current induced dissipation of heat) and falling within the expected range at the wind speeds observed in our study, as suggested by Raymond and Cole (2001).

We calculated the air–water fluxes of gases separately for when water was in-channel and over the marsh because wind speed is likely to be substantially different at the

bottom of a *S. alterniflora* canopy vs. over an open waterbody. Over open water, we used the average wind speed during each dawn-dusk interval. Wind was assumed to be still (0 m s^{-1} wind) at the air–water surface within the marsh canopy. Thus, we used the intercept value for K_T when the marsh was flooded.

Areal rates of gas flux were determined taking into consideration the areas of "open water" and flooded marsh as determined from ArcMap and the detailed GCE-LTER vegetation-corrected digital elevation model (DEM). The "open water" surface area (See in Supporting Information Appendix B—Open Water Mid-tide Area Table) was determined for each segment at its mid-tide location (Supporting Information Appendix A) and elevation (0 MSL). The flooded marsh area (see in Supporting Information Appendix B—Flooded Marsh Area Table) was also measured for each segment based on the observed high tide level during each sampling interval. We used half of the maximum marsh area flooded to represent the average amount of marsh flooded during each 6 h interval when water level is ≥ 0 MSL. Further details on calculating air–water exchange surface areas are described in Supporting Information Appendix B.

Longitudinal mixing

The longitudinal mixing or dispersion (M in Eq. 1) is calculated as the product of the horizontal dispersion coefficient (ε, m^2 s^{-1}), the along-stream concentration gradient (δ[DIC (DO)]/δx) and cross-sectional area A_c for each sampling segment:

$$M = \varepsilon * \delta[\mathrm{DIC\,(DO)}]/\delta x \quad (4)$$

A cross-sectional area of 979 m^2 was estimated from a high resolution DEM (Mcknight 2016). As there is an extreme paucity of information on effective dispersion coefficients for meso-tidal salt marsh estuaries, we used the value determined by Imberger et al. (1983) for the upper Duplin River following a rainstorm freshening event and ramped it up towards the ocean as determined by Vallino and Hopkinson (1998) for the very similar upper 15 km of the Parker River estuary using water mass tracers and hydrodynamic modeling. In our study, ε ranges from 27.4 m^2 s^{-1} to 35.9 m^2 s^{-1}, increasing downstream along the length of the Duplin. The equation we used to calculate the change in dispersion along the length of the Duplin is shown in Supporting Information Appendix C.

Metabolism

Metabolism is calculated for each station segment (1 km long) along the Duplin River as the balance between the diurnal rate of change in masses of DIC and DO, air–water exchange and longitudinal mixing across each segment boundary (Eq. 1). Following Odum's convention (1956) the balance calculated between sunset and sunrise is defined as ecosystem respiration (R) and the balance between sunrise and sunset is defined as net daytime production (NDP). NDP reflects the balance between gross primary production (GPP) and R:

$$\mathrm{NDP} = \mathrm{GPP} + R \quad (5)$$

Assuming the rate of R measured at night holds throughout daytime, GPP is calculated as NDP + R (during daytime hours only).

Recalling that the water in the Duplin River is our reference system, GPP is a positive number with respect to the O_2 mass balance, as it adds O_2 to the water, and GPP is a negative number with respect to the DIC mass balance, as it removes DIC from the water. Similarly, R is a negative number for O_2 consumption and a positive number for DIC production.

Daily NEP reflects the balance of GPP and R for 24 h:

$$\mathrm{NEP}\left(\mathrm{mol\,d^{-1}}\right) = \mathrm{GPP} * \mathrm{Daytime\,h} + R * 24\,\mathrm{h} \quad (6)$$

We report metabolism in several ways.

Spatial distribution

Metabolism of each 1 km long segment per unit volume along the Duplin (mol m^{-3} d^{-1}) = daily metabolism of each segment (mol d^{-1}) divided by the water volume of each segment (m^3) (See in Supporting Information Appendix B—Duplin River Segment Volumes Table).

Seasonal pattern

Seasonal daily areal rates of metabolism for the entire Duplin salt marsh-estuary (mol m^{-2} d^{-1}) = sum of the daily metabolism for the 12 segments divided by the annual averaged total water area, which is 2.1 × 10^6 m^2 at mean high water (MHW) (1.0 m).

Annually

Annual metabolism for the entire Duplin River salt marsh-estuary = averaged seasonal daily areal rates * 365 d * the annual average total water area 2.1 × 10^6 m^2.

The RQ (CO_2 produced/O_2 consumed through respiration) and PQ (O_2 produced/CO_2 consumed through primary production) were calculated for the entire Duplin seasonally using the median of values calculated for each of the 12 Duplin River water mass segments.

Estimation of the marsh contribution to entire salt marsh-estuary metabolism

While for most of the tidal cycle and dawn-dusk interval the Duplin River water is within channel, during at least part of the tidal cycle, water floods over creek banks onto the marsh platform. Thus, some aspects of marsh metabolism are incorporated into metabolism as measured in the water. To quantify the contribution that the marsh makes to the entire Duplin River marsh-estuary ecosystem metabolism, we separately measured the net horizontal transport

flux of DIC and O_2 and estimated air–water exchange during marsh inundation. The balance between the net transport and the air–water exchange is a measure of marsh metabolism. We extrapolated results for the single tidal creek study to the entire Duplin salt marsh-estuary by taking into consideration the relative areas of marsh flooded during our seasonal sampling trips.

The net horizontal transport of DIC and DO in and out of the small tidal creek that floods the flux tower marsh platform, $Q_{M\text{-}H}$, is estimated as the product of water transport ($m^3\ s^{-1}$) and [DIC] or [DO] over an entire tidal cycle.

$$Q_{M-H} = \int_{LT_1}^{LT2} [\mathrm{DIC}\,(\mathrm{DO})](t) * \text{transport}\,(t) * \mathrm{d}t \qquad (7)$$

Where LT1 and LT2 are the times when a tidal cycle started at the first low tide and ended at the next low tide. Samples for DO and DIC concentration analysis were collected at the mouth of the tidal creek 1/2-hourly for a complete tidal cycle, the day after the Duplin dawn-dusk transects were conducted. In the winter, we conducted a second flux study when tides were higher (18 March), because less than 10% of the marsh was flooded during the February trip. Tidal creek sampling was conducted only when high tide occurred during daylight.

Water transport was determined as the quarter-hourly changes in water storage (ArcMap) in the tidal creek and its catchment over a complete tidal cycle. Water transport in the thalweg of the tidal creek was measured with an Acoustic Doppler Current Profiler (ADCP), but because it missed water entering the catchment directly from the Duplin via overbank, marsh sheetflow flooding, we considered the approach inadequate for our purposes.

The ArcMap 10.2.2 Surface Volume Functional Surface Tool was used to estimate volume for 15 min records of tidal height within the tidal creek catchment. The catchment boundaries were defined by field surveys of where adjacent creek waters met at high tide for the northern and eastern boundary, by the top of the natural levee along the Duplin River to the west, and by a location midway to the adjacent tidal creek to the south. The change in volume over 15 min was used to develop water transport as a function of tidal stage, transport (t) in Eq. 7. Our ArcMap layers were the high precision (2 cm), vegetation corrected (Hladik and Alber 2012) Duplin River marsh DEM and water levels recorded in the tidal creek (GPS surveyed and tied into local MSL) by the GCE-LTER.

The vertical transport $Q_{M\text{-}v}$ across the flooding marsh water surface was estimated as the product of air–water flux over the tidal creek (F_{tc}) and the inundated marsh area (A_{tc}) over an entire tidal cycle:

$$Q_{M-v}\,(\mathrm{mol\,tide^{-1}}) = \int_{LT1}^{LT2} F\mathrm{tc}(t) * A\mathrm{tc}(t) * \mathrm{d}t \qquad (8)$$

F_{tc} was estimated the same way as described in Eqs. 2, 3, except that, rather than measure pCO_2, we calculated it with the online CO_2 system calculation tool—CO2SYS_V2.1.xls (http://cdiac.ornl.gov/ftp/co2sys/CO2SYS_calc_XLS_v2.1/) with measured DIC and Alk from the discrete water samples collected 1/2 hourly during the rising and fall tide. We assumed still winds at the base of the marsh grass canopy in our calculation of the gas transfer velocity, K_T. The inundated area A_{tc} as a function of tidal stage was also determined with the ArcMap 10.2.2 Surface Volume Functional Surface Tool with 15 min records of tidal height within the defined catchment.

The net daytime production, NDP_{marsh}, of the inundated marsh (including platform, creek bank, and water components) was calculated as the net tidal horizontal transport of DIC or DO from the tidal creek catchment ($Q_{M\text{-}H}$) corrected for the vertical air–water transport ($Q_{M\text{-}V}$).

$$\mathrm{NDP_{marsh}} = Q_{M-H} + Q_{M-V} \qquad (9)$$

Areal rates of lateral transport, vertical transport, and metabolism were calculated by dividing $Q_{M\text{-}H}$, $Q_{M\text{-}v}$, and NDP_{marsh} by the average flooding area of the tidal creek catchment during each sampling trip. The average was calculated as 1/2 the maximum area flooded for each sampling tide: 2600 m^2, 21,500 m^2, 11,000 m^2, 21,800 m^2, and 21,500 m^2 for February, March, May, August, and October, respectively. To express the relative contribution of marsh NDP to metabolism of the entire Duplin salt marsh-estuary, we scaled results on the basis of two flood tides per day and the relative extent of marsh in the small tidal creek catchment compared to the area of marsh flooded by "resident" water for the entire Duplin.

Results

Environmental conditions during the study

Our sampling design enabled us to capture the full seasonal range of metabolically significant physical and ecological drivers likely to control ecosystem metabolism in the Duplin River system (Table 1). Water temperatures during our sampling trips were within a standard deviation of the 10-yr seasonal averages for each season, ranging from a low of 13.6°C in winter (February) to a high of 30.0°C in summer (August). Similarly, we captured the full seasonal range in solar insolation, although being less than average during our cloudy February sampling (11.7 mol $m^{-2}\ d^{-1}$) and slightly above average during our cloud-free May sampling (44.8 mol $m^{-2}\ d^{-1}$). Variations in salinity reflect primarily variations in Altamaha river discharge. Wind speed was low and stable for our trips with a mean value of 3.0 ± 0.4 m s^{-1}, compared with the 10-yr mean value of 3.8 ± 0.5 m s^{-1}. Chlorophyll *a* concentrations ranged from a seasonal low of 6.9 μg L^{-1} in February to a high of 13.6 μg L^{-1} in May and were within a standard deviation of the 10-yr mean for each season. DOC

Table 1. Physical and ecological conditions observed in the Duplin River salt marsh-estuary in 2014. Seasonal means and standard deviations were calculated by averaging 2002–2011 monthly water quality, meteorological, and nutrient data collected at either Marsh Landing (Sta. 0) or Hunt Dock (between Sta. 8 and 9) by the Sapelo Island National Estuarine Research Reserve and the GCE-LTER. In situ data were collected during our four field trips. Where data are available for multiple stations, values reported represent the arithmetic mean.

Sampling season	Sampling month	Salinity PSU (in situ)	Water temperature °C		PAR (mol m^{-2} d^{-1})		Wind speed (m s^{-1})		Chl (μg L^{-1})		DOC (μmol L^{-1})
			Mean	In situ	Mean	In situ	Mean	In situ	Mean	In situ	In situ
Winter	Feb	21.3	12.8 ± 2.4	13.6	19.3 ± 3.7	11.7	3.6 ± 0.6	3.4	8.3 ± 1.9	6.9	323
Spring	May	19.2	20.3 ± 4.1	23.2	36.7 ± 6.7	44.8	3.9 ± 0.5	3.3	7.4 ± 1.4	13.6	380
Summer	Aug	26.8	29.0 ± 1.5	30.0	38.3 ± 5.6	35.8	3.8 ± 0.4	2.9	11.9 ± 2.7	10.2	428
Fall	Oct	28.9	22.6 ± 4.6	22.8	26.1 ± 5.8	33.3	3.7 ± 0.5	2.6	7.9 ± 1.4	8.6	375

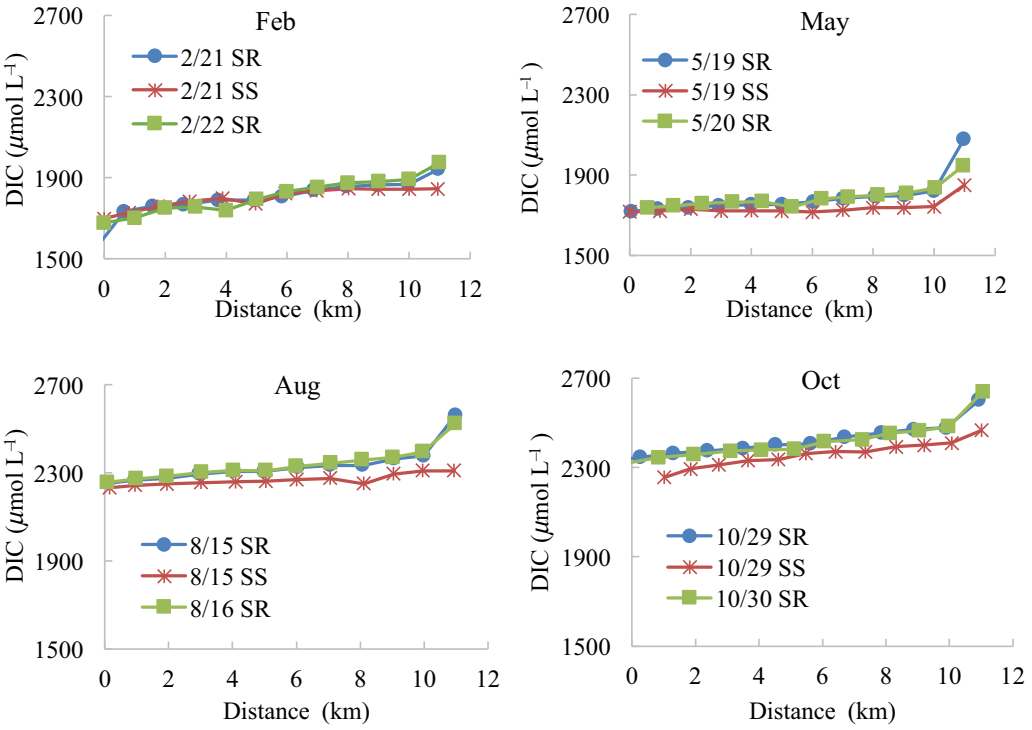

Fig. 2. Diurnal DIC along the Duplin estuary for each season: For each trip, measurements were taken at sunrise (SR), sunset (SS), and the next sunrise at 12 stations equally spaced 1 km apart along the river.

concentrations were similar to previous reports (Sottile 1973; Imberger et al. 1983) showing little annual variation (323–428 μmol L^{-1} DOC). There are no long-term data available for DOC in this system. The close adherence to seasonal trends observed through long-term monitoring suggests that carbon and oxygen dynamics and ecosystem metabolism we observed over the course of 2014 are typical and adequately captured seasonal patterns.

Seasonal and spatial patterns for DIC, pCO_2, and DO in the Duplin River

We observed similar spatial, seasonal, and diurnal patterns for pCO_2 and DIC along the length of the Duplin River that were inverse the patterns for DO. The DIC distribution along the Duplin River was similar during all months (Fig. 2): typically increasing with distance upriver and away from the ocean especially in the final kilometer. Overall, levels were lowest in the coldest month (February), increasing from about 1600–1700 μmol L^{-1} at the mouth to 1850–1950 μmol L^{-1} at the head. Concentrations of DIC reached their highest levels in the warmest months (August and October), increasing from about 2200–2350 μmol L^{-1} at the mouth to as high as 2650 μmol L^{-1} at the head. The up-estuarine gradient was about 250 μmol L^{-1} in February but increased to 350–400 μmol L^{-1} in the warmest months. There was also a strong diurnal signal, with values highest just after sunrise and

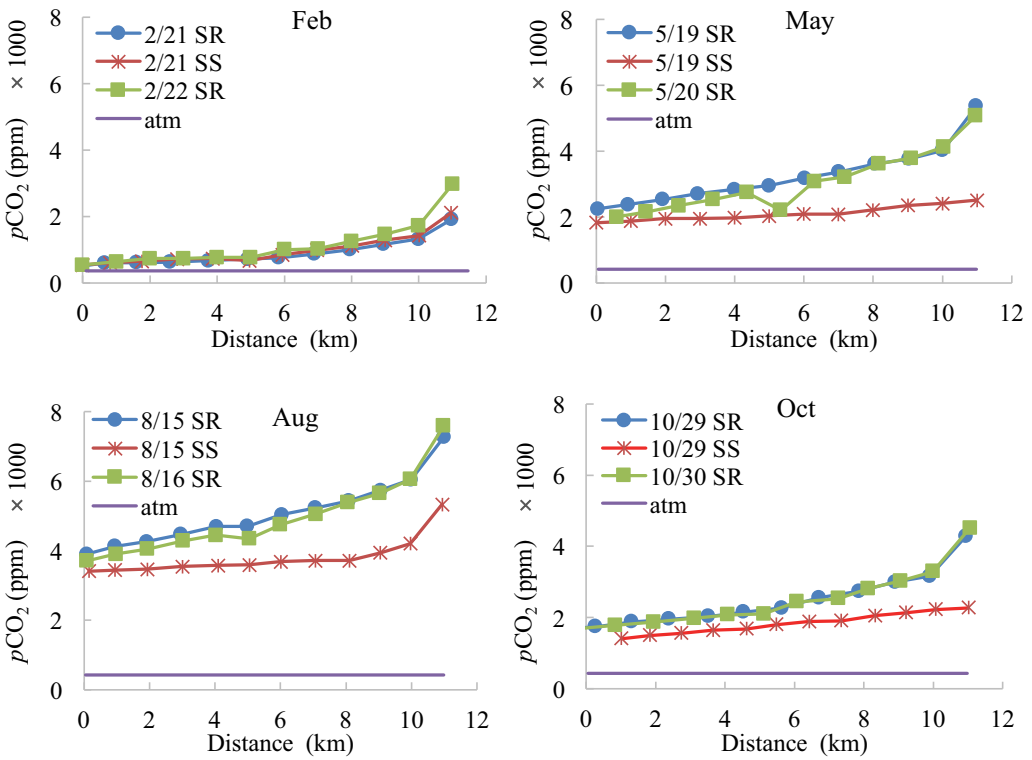

Fig. 3. Diurnal partial pressure of CO_2 (pCO_2) distribution along the Duplin estuary for each season: the straight line is the average measured pCO_2 level in the atmosphere.

lowest in late afternoon at sunset. The diurnal range in values was least in February (25–100 μmol L^{-1}) and greatest in August (up to 300 μmol L^{-1}). The diurnal range was also greater at the head of the estuary than it was near the mouth. The positive up-estuary gradient in DIC shows that the estuary is a source of DIC to the coastal ocean year-round and is particularly so during late summer and early fall. The increase in diurnal amplitude up-estuary suggests that metabolic activity increases up the estuary and during the warmer months of the year. These conclusions are consistent with the earlier studies that are summarized in Cai (2011).

Duplin pCO_2 had spatial, diel and seasonal patterns similar to DIC (Fig. 3). Overall pCO_2 levels were lowest in the coldest month (February), increasing from about 500 ppm at the mouth to 3000 ppm at the head, and highest in the warmest month (August), increasing from 3500 ppm at the mouth to 7500 ppm at the head. The diel difference in pCO_2 was most prominent in May and August and least prominent in February. Throughout the year, pCO_2 levels for all stations were higher than in the atmosphere (400 ppm), showing that waters of the Duplin River estuary were a net source of CO_2 to the atmosphere year-round.

DO distributions were typically inverse those observed for inorganic carbon (Fig. 4). For most transects, DO typically decreased with distance upriver and away from the ocean especially in the last kilometer and for sunrise transects. For each station, the diurnal range was greater at the head of the estuary than it was near the mouth. The 100% saturated DO levels along river varied by month and with distance upriver in accordance with seasonal patterns in temperature and salinity (Table 1). Duplin water was under-saturated in DO year-round especially upriver and during the warmest month of the year August. The annual and diurnal spatial patterns of DO under-saturation suggest that the Duplin River is a net sink of atmospheric O_2 year-round and that metabolic activity increases up the estuary and during the warmest months of the year.

DIC and DO tidal exchange in the small tidal creek

DIC concentrations in the small tidal creek varied substantially over a flood-ebb tidal cycle but minimally from season to season (Fig. 5a). During all seasons the tidal pattern was similar: high DIC concentration at low tide (ranging from 2500 μmol L^{-1} in March to 4300 μmol L^{-1} in August), a sudden drop as creek bank drainage water was replaced with low DIC water flooding in from the Duplin, low concentrations near high tide (ranging from 1500 μmol L^{-1} in February to 2250 μmol L^{-1} in October), and a slow continual rise during ebbing tide back to initial levels. The greatest difference between high and low tide DIC concentrations was in August when metabolism of the flooded

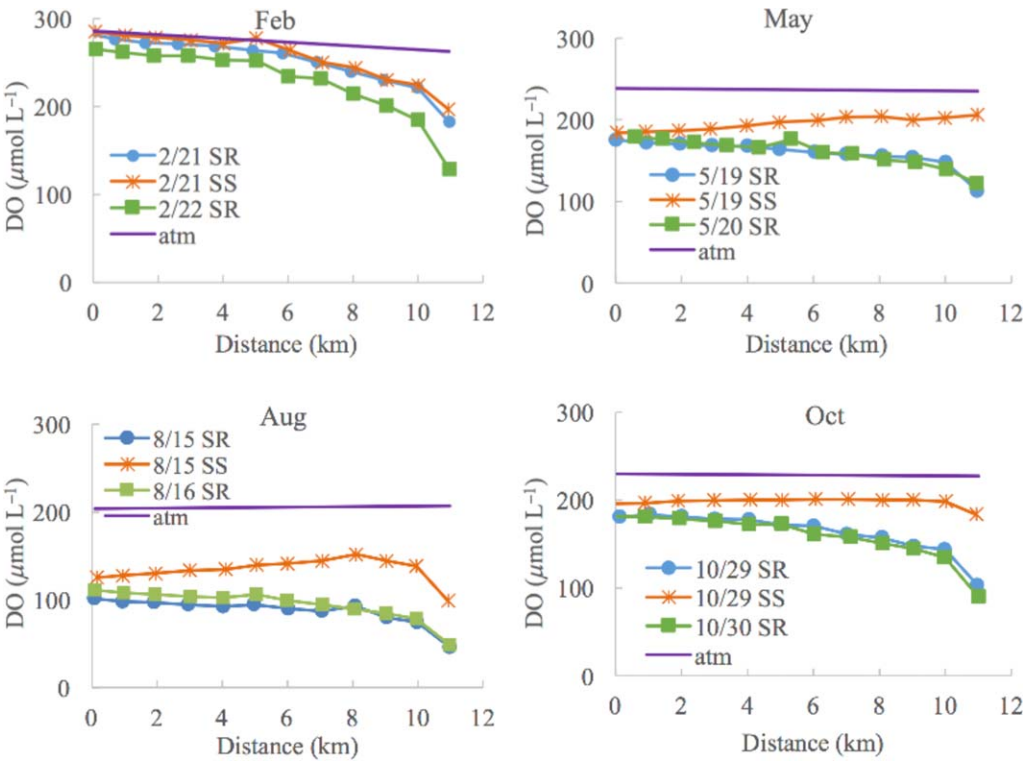

Fig. 4. Diurnal dissolved O_2 (DO) distribution along the Duplin estuary for each season. The straight line is the 100% saturated DO level.

marsh community was expected to be most active. We note that the marsh platform is typically completely drained within 3 h of high tide, thus much of the DIC draining during the final stages of the ebb tide likely originates from drainage of creek bank pore waters (sensu Gardner and Gaines 2008). The total length of creekbank edge upstream of where we collected samples is 862 m.

Calculated pCO_2 levels in tidal creek water showed tidal and seasonal patterns similar to DIC (Fig. 5b). pCO_2 in the tidal creek dropped rapidly as Duplin River water entered the tidal creek, remained relatively low during high tide and then rebounded during marsh platform and creek bank porewater drainage. The change between low tide and high tide was most prominent in August and least prominent in February. Overall pCO_2 levels were lowest in the coldest month (February), ranging from 500 ppm at high tide to 4000 ppm at low tide, and highest in the warmest month (August), ranging from 1600 ppm at high tide to 12,000 ppm at low tide. Throughout the year, pCO_2 levels in the tidal creek were higher than in the atmosphere (400 ppm), showing that tidal creek water was a net source of CO_2 to the atmosphere, especially the final portion of water draining from creek banks in the summer.

The seasonal and tidal patterns of DO concentrations in the small tidal creek were typically inverse those observed for DIC and pCO_2 (Fig. 5c). For each sampling month, the low DO concentration at low tide typically had a sudden jump as high-DO water flooded into and onto the marsh from the Duplin. The pattern thereafter varied seasonally, sometimes reaching highest levels prior to high tide near midday (e.g., May and August) and sometimes several hours after high tide, as in October. As with inorganic carbon, DO slowly returned to initial low tide values. Only once during our study did we observe super-saturated levels of DO in tidal creek water. In October, concentrations increased after high tide reaching a level of 240 μmol L^{-1} (vs. a saturation level of 220 μmol L^{-1}). Total PAR reaching flood tide waters was higher in October than any other month (data not shown). During the October trip, the timing of high tide most closely coincided with peak PAR at midday and the October trip was cloud-free.

Water transport estimation in the small tidal creek

Volume transport and catchment area flooded were directly related to high tide water level (Table 2). High tide water levels and the resultant areal extent of marsh flooded varied substantially during our five sampling trips. In February, high tide reached just over 0.8 m (MSL), while in March it exceeded 1.3 m (MSL). The amount of marsh flooded increases rapidly once water level reaches the marsh platform at about 0.8 m (MSL). With a 0.84 m water level in February only 4494 m^2 of marsh was flooded, while at 0.95 m in May over 20,000 m^2 was flooded. Once water level reached about 1.2 m, the entire tidal creek catchment of

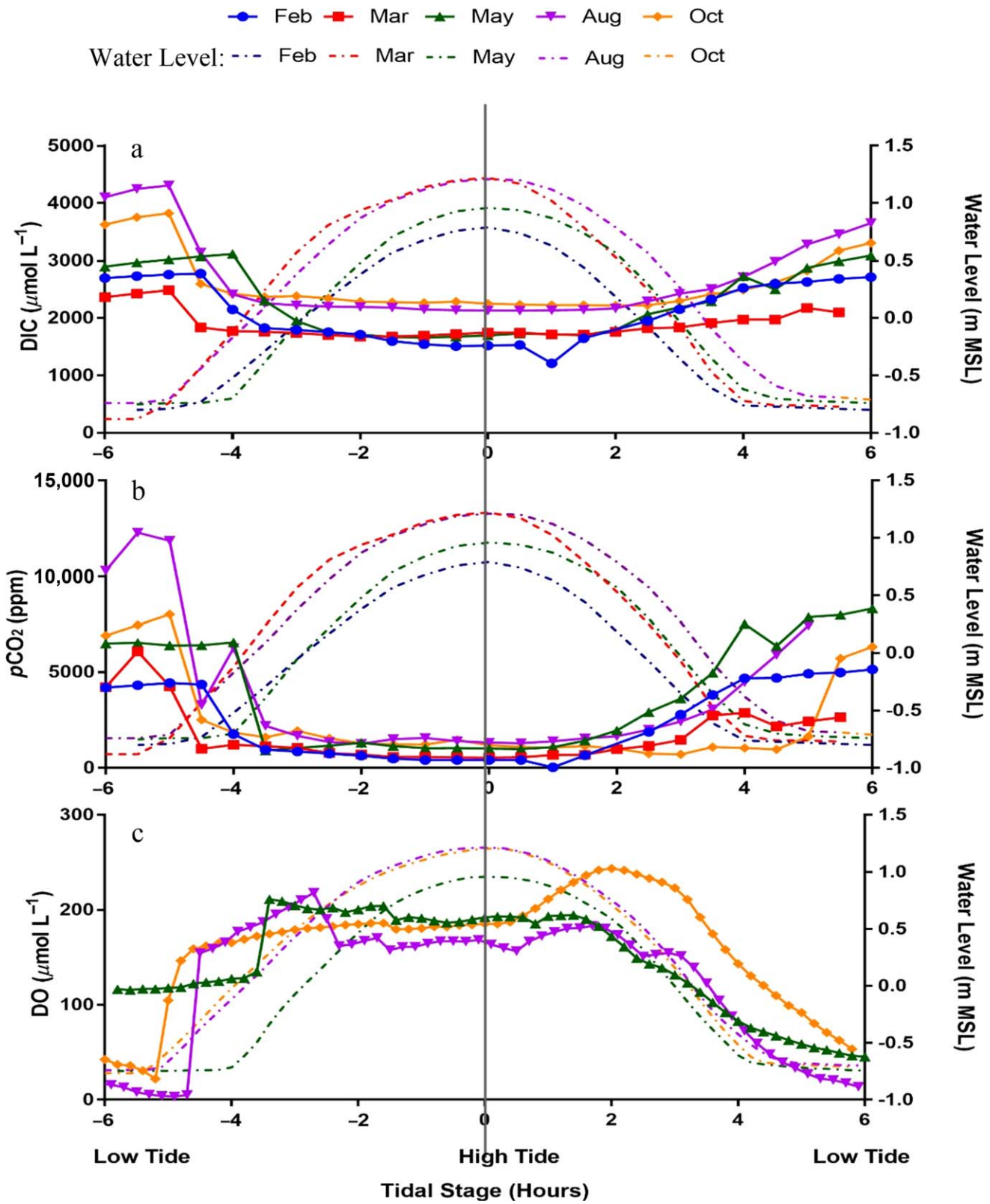

Fig. 5. (a) DIC, (b) partial pressure of CO_2 (pCO_2) and (c) dissolve O_2 (DO) concentrations (solid lines) and water levels (dashed lines) over a tidal cycle at the small tidal creek: Water depth is relative to 0 m MSL. The elevation of the marsh platform here ranges from about 0.8–1.2 m. At levels less than 0.8 m, all water is confined within the tidal creek, which is up to 20 m wide and heavily vegetated except for about a 2 m wide thalweg. We did not collect DO data in February and March.

Table 2. Water level, volume transport, and flooded area estimation for the small tidal creek during our sampling.

Month	High tide water depth (m)	Flood/ebb volume (m^3)	Max flood area (m^2)
Feb	0.84	1132	4494
Mar	1.34	18,341	43,327
May	0.95	2282	20,178
Aug	1.17	10,299	43,327
Oct	1.20	11,617	43,327

43,327 m^2 was flooded. This occurred in March, August, and October.

Water transport volumes in the small tidal creek were proportional to water level and ranged from as little as 1132 m^3 per flood and ebb tide in February to 18,341 m^3 in March. Transport was twice as high in May (2282 m^3) as in February and was 10,229 and 11,617 m^3 in August and October (Table 2).

With each tidal cycle, there is a complete draining of all water that enters during flood tide, thus there is a zero-net flux of water for a tidal cycle. The exception to this would be if there was significant evaporation or rainfall during the tidal cycle. Under certain wind conditions, it is also likely that small tidal creek water mixes with water from adjacent tidal creeks. However, all our observations were conducted on relatively low wind days, so exchange with adjacent creeks was likely minimal.

Discussion

Air–water exchange

The spatial distribution of air–water fluxes was similar to that for the along-estuary distribution of pCO_2 and DO, with increasing exchange rates from the mouth to headwaters (Figs. 3, 4). The seasonal pattern of air–water exchange was similar for the two gases: strongest in August and weakest in February (Fig. 6). The seasonality reflects the deviation from saturation values, which in turn is related to the balance between mixing and ecosystem metabolism. Deviation from saturation values is greatest in summer and least in winter (Figs. 3, 4) because of the effect of temperature on solubility and temperature and light on rates of photosynthesis and respiration.

We calculate that areal gas exchange fluxes from channel water (-0.7 mmol CO_2 m^{-2} h^{-1} to -5.5 mmol CO_2 m^{-2} h^{-1}, 0.6 mmol O_2 m^{-2} h^{-1} to 4.5 mmol O_2 m^{-2} h^{-1}) are higher than from flooded-marsh water (-0.6 mmol CO_2 m^{-2} h^{-1} to -3.9 mmol CO_2 m^{-2} h^{-1}, 0.5 mmol m^{-2} h^{-1} to 3.7 mmol m^{-2} h^{-1}) (Fig. 6a, c). This is a direct result of our assumption that wind speeds within the marsh canopy during marsh flooding are still, thus the gas transfer velocity, K_T, used to calculate air–water exchange is low for the marsh overlying water (the wind speed vs. K_T intercept value: 3 cm h^{-1}) and invariable with respect to wind velocity.

DO and CO_2 fluxes are almost mirror images for each other—CO_2 to atmosphere and O_2 to the Duplin River. On average, rates of CO_2 flux are about 20% higher than for O_2, ranging from as little as 6% to as much as 30% higher. This near balance of O_2 and CO_2 fluxes in estuaries with high pCO_2 was also observed in the marsh-dominated Satilla River estuary (Cai and Wang 1998; Cai et al. 1999). In low pCO_2 estuarine and coastal waters, this is often not the case (Zhai et al. 2009; Omstedt et al. 2014).

The seasonal pattern of the total air–water exchange of CO_2 and DO followed the same seasonal pattern observed for areal rates in either marshes or channel waters, but the relative importance of gas fluxes over the marshes and open channel waters differs (Fig. 6b,d). This is because the flux when water is over the marsh reflects not only the amount of time the marsh was flooded but also the absolute area of marsh flooded. This changes as a function of tide height, which varies twice daily, forth-nightly in conjunction with the spring-neap tidal cycle and seasonally in relation to coastal climatology. Marsh surface water accounted for 14–36% of the total CO_2 flux and 16–39% of the total O_2 flux depending on corresponding areal gas exchange rate and inundation area and duration. Considering the relative importance of this process that occurs for a short interval but over such a large area, it is remarkable how limited our understanding is of the mechanisms controlling gas exchange from flooded wetland surfaces. Although our equation for transfer velocity includes a nonzero intercept to account for the K_T in a zero-wind speed situation, it is still insufficient to capture processes such as canopy characteristics (Lightbody and Nepf 2006), buoyancy (Fairaill et al. 2000), surface-water turbulence (Zappa et al. 2007), rain (Ho et al. 2004), etc., that may dominate vertical gas transfer in a non-wind condition. Future studies on generating models based on non-wind factors would enable us to better understand gas flux across the air–water boundary for a wetland.

Annually, the entire Duplin system degassed 7.4×10^7 mol yr^{-1} of CO_2 to the atmosphere and absorbed 6.1×10^7 mol yr^{-1} of O_2 from the atmosphere, of which one third of these fluxes occurred over the inundated marsh water surface. To express these fluxes in mol m^{-2} yr^{-1}, 18 mol CO_2 m^{-2} yr^{-1} was lost and 15 mol O_2 m^{-2} yr^{-1} was gained across the entire Duplin's air–water surface.

Mixing with coastal water

The Duplin estuary exported DIC and imported DO to and from Doboy Sound and the coastal ocean during each sampling trip in all four seasons of the year (Fig. 7). The Duplin exported DIC at high rates in February and October to Doboy sound (10.3×10^4 mol d^{-1} and 15.1×10^4 mol d^{-1}) and at lower rates in May and August (2.7×10^4 mol d^{-1} and 3.4×10^4 mol d^{-1}) (Fig. 7a), reflecting the seasonal

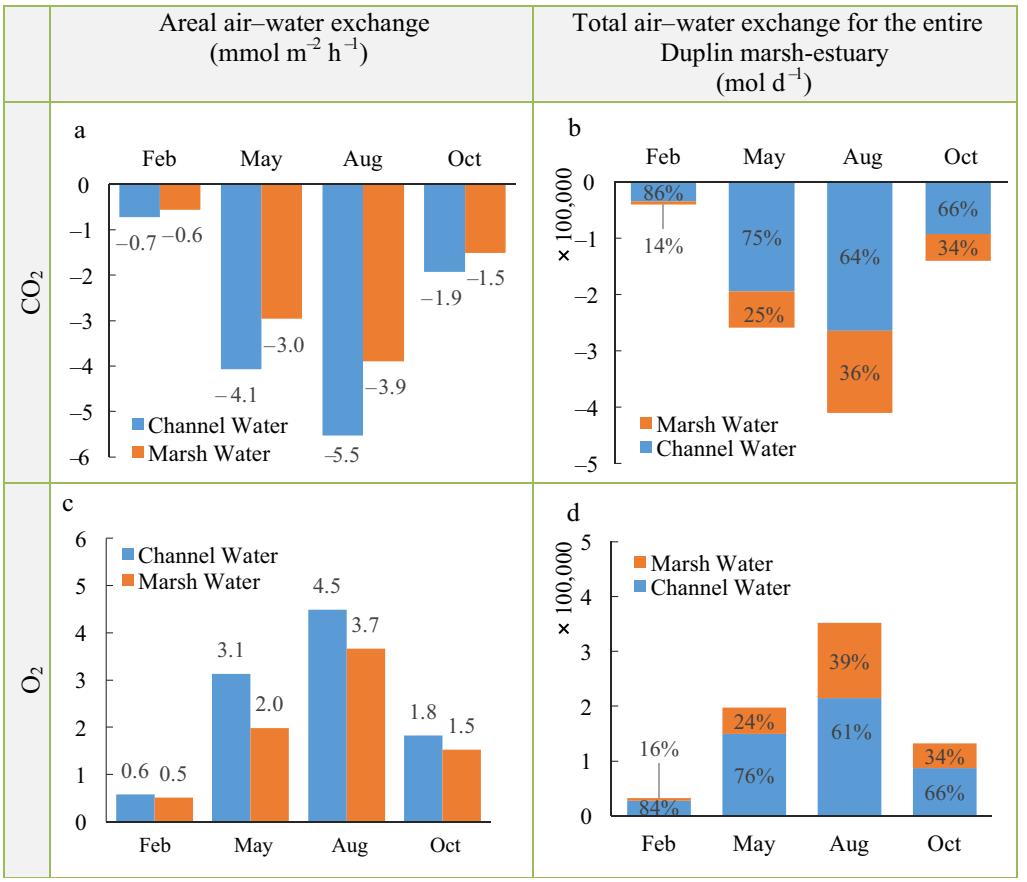

Fig. 6. Seasonal air–water exchange for open water and flooded marsh zones: (**a**) Areal air–water flux of CO_2. (**b**) Total daily air–water CO_2 exchange scaled to the entire Duplin system. (**c**) Areal air–water flux of O_2. (**d**) Total daily air–water O_2 exchange scaled to the entire Duplin system.

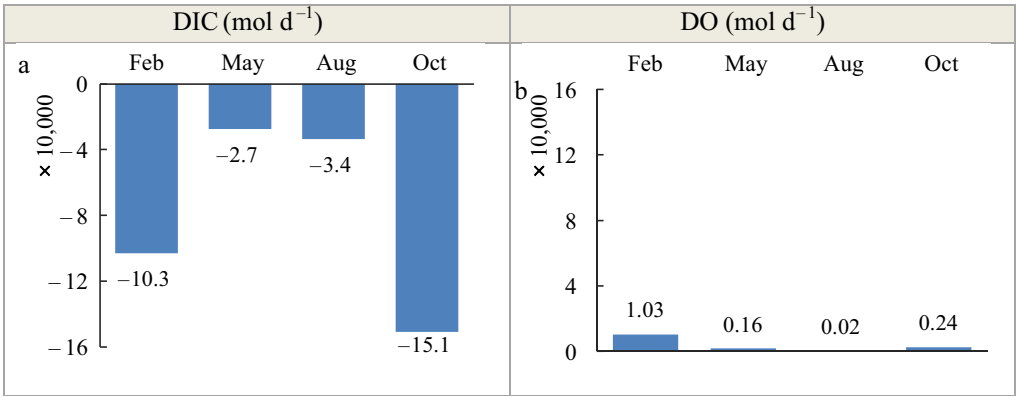

Fig. 7. Seasonal mixing between the Duplin estuary and coastal water: (a) daily DIC and (b) dissolved O_2 (DO) exchange at the mouth of the Duplin estuary with the adjacent coastal waters of Doboy Sound and the ocean. Negative transport represents export from the Duplin to coastal water, and positive transport represent import from the coastal water to the Duplin.

variation in the along-estuary DIC gradient (Fig. 2). The Duplin imported DO from Doboy sound and coastal water year-round, but to a much lower extent compared to DIC export (Fig. 7b), ranging from 0.02×10^4 mol d^{-1} in August to 1.0×10^4 mol d^{-1} in February. While the seasonality was similar for DIC and O_2, they differed by at least an order of magnitude. This inconsistency in the mixing of the two gases with coastal water is interesting and requires further study. We note that as the air–water flux of CO_2 and O_2 dominates the total exchange with adjacent systems

(atmosphere and oceanic water), the combined total exchange does not disagree greatly. We suggest that this inconsistency is a result of a greatly imbalanced ratio of air–water exchange surface (channel and flooded marsh 4.1×10^6 m^2) relative to a very limited channel cross-sectional area through which mixing occurs (979 m^2).

The temporal pattern of mixing of DIC and DO is opposite in direction to the air–water flux (Fig. 7). This pattern may reflect the balance between metabolism, air–water exchange, and mixing. Net ecosystem metabolism (NEP) should have a similar seasonal pattern as air–water flux since they are both mainly driven by temperature variation. Thus, air–water flux dominates total system loss or gain of the metabolic gas, whereas the lateral transport to coastal water reflects the residual after correcting for the vertical transport. This may partially explain why the lateral transport showed the opposite temporal pattern to air–water flux.

Integrated annual DIC export from the Duplin River to the coastal ocean was estimated as 2.9×10^7 mol yr^{-1}, which is about three times higher than a previous estimate of 0.96×10^7 mol yr^{-1} (Wang and Cai 2004). Our more accurate estimation of cross-sectional area for the Duplin mouth (979 m^2 vs. Wang's 654 m^2 from Imberger et al. 1983) and our refined model of how dispersion increases along the length of the Duplin estuary (vs. a uniform and lower ε from Imberger et al. 1983) certainly contribute to the difference in estimates. In addition, our estimate of the concentration gradient is based on the concentration between adjacent water masses at the mouth of the Duplin, whereas Wang and Cai used a gradient that ranged from the upper reaches of the Duplin at low tide to the oceanic water at the mouth of the Duplin at high tide.

The combined air–water exchange and horizontal dispersion mixing flux of inorganic C from the Duplin system was 25 mol C m^{-2} yr^{-1} to adjacent systems, of which 72% was to the atmosphere and 28% was to the coastal ocean. The gain of O_2 from adjacent oceanic and atmospheric systems was 15 mol m^{-2} yr^{-1}, which is smaller than the loss of C, mainly due to the much lower longitudinal mixing of O_2. The total loss of inorganic C from the Duplin salt marsh estuary is about two times larger than the 8.3 mol m^{-2} yr^{-1} estimated for the York River estuary, within the Chesapeake Bay system (Raymond et al. 2000). This may reflect the much smaller ratio of marsh to river area and the greater freshwater input in the York compared to the Duplin. However, the degassing flux in the Duplin River is similar to that of the upper and mid parts of the Satilla River estuary, a Georgia riverine estuary with a similarly large marsh to open water ratio but a much greater freshwater input (Cai and Wang 1998).

Metabolism of the Duplin salt marsh-estuary

The environment that contributes to the metabolism measured by the open water approach includes the water column and permanently flooded subtidal benthos, the intermittently flooded intertidal flats and creek banks below MSL, and the marsh creek banks and platform above MSL. Autotrophic communities include phytoplankton in the water column, benthic micro algae on creek bottoms, banks and marsh platform and perhaps those portions of emergent marsh macrophytes that are flooded at high tide. Communities that contribute to respiration other than the autotrophs include heterotrophic plankton and mobile macrofauna in the water column, benthos of creek bottoms, creek banks and marsh surface, aufwuchs associated with live and dead-standing marsh macrophytes and perhaps flooded portions of marsh macrophytes. Quite likely the open water technique measures some aspects of intertidal marsh respiration that occurs even when the marsh is not flooded, as DIC, DOC, and other dissolved metabolites (e.g., HS^-) that build up to extremely high concentrations in marsh sediments (Koretsky et al. 2003; Neubauer and Anderson 2003) diffuse into overlying flood waters during high tide or drain from creekbanks into creek waters at low tide (Raymond and Hopkinson 2003; Gardner and Gaines 2008). Our definition of aquatic salt marsh-estuarine metabolism needs to include not only estuarine water bodies and their sediments, but also some portion, in space and time, of the intertidal marshes. This blending of the marsh with estuarine creeks, bays, and sounds blurs the lines between how salt marsh estuaries have been conceptualized historically in text books and the literature.

There was a pronounced spatial pattern of metabolic activity that held from season to season for both CO_2 and O_2 approaches (Figs. 8, 9): community respiration and GPP typically increased two to fivefold and uniformly with distance along the Duplin, then abruptly increased up to tenfold in the final kilometer. Exceptions to this pattern were seen in October for C-based metabolism (Fig. 8), where GPP and R actually slightly decreased along the 4.5 km from the mouth of the estuary, then increased until the final station. Such results were not seen with oxygen (Fig. 9), however, as metabolism increased two to threefold up-estuary in October. The upstream enhancement of metabolism most likely reflects gradients in marsh density (marsh area/channel water area, see Cai et al. 1999), temperature, inorganic nutrient concentrations, DOC, and Chl *a* (Wiegert et al 1981). Water residence time is also longer in the upper estuary (Mcknight 2016), which promotes the accumulation of materials upstream. The marsh has been shown previously to be a source of DOC and DIC to estuarine waters (Sottile 1973; Imberger et al. 1983; Peterson et al. 1994; Wang and Cai 2004), which is likely to be enhanced in the upper portion of the Duplin River where the drainage density of tidal creeks and flooding extent is highest (Frey and Basan 1978; Wadsworth 1980). Along the Duplin, *R* was consistently greater than GPP indicating that the system was net heterotrophic during all seasons. Thus, more DIC was produced than consumed and vice versa for DO—more O_2 consumed

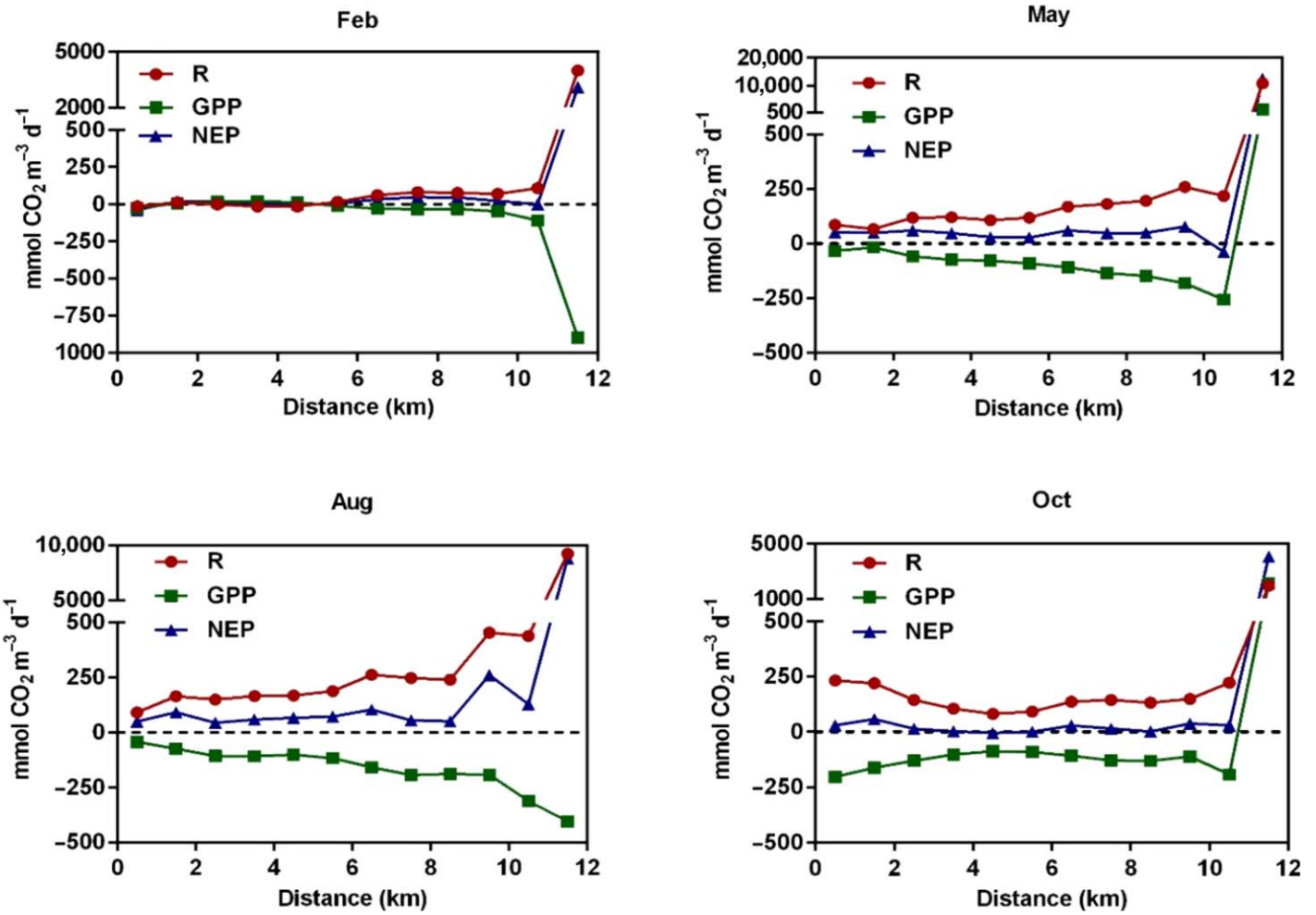

Fig. 8. Distribution of metabolic rates calculated from changes in DIC (labeled CO_2) along the Duplin River estuary.

than produced. These patterns are consistent with our observations that the Duplin was a source of CO_2 to the atmosphere and a sink for O_2, and thus dependent on allochthonous organic matter to fuel the respiration in the excess of GPP.

An exception to the pattern of increasing GPP with distance up estuary was seen at the upper-most station (Figs. 8, 9). GPP became negative (DIC production and O_2 consumption) during two seasons for dissolved inorganic C and three seasons for DO. This is unexpected and unrealistic. It occurred during the warmer times of the year, which leads us to suspect a diurnal temperature effect on respiration as described by Tobias et al. (2007) using oxygen stable isotopes—enhanced during the day when flooding a hot marsh surface exposed to full sunlight and reduced at night, when tidal water likely cooled during marsh inundation. The open water approach calculates GPP as NDP measured during the day adjusted for respiration measured at night. If temperature enhances respiration during the day, then we underestimate the respiratory correction of NDP. We timed our field trips so that our dawn sampling was close to low tide, thus high tide would have occurred when marsh surface temperatures were greatest. This effect was seen only in the final kilometer of the Duplin, because the entire low tide volume of that reach moves onto the marsh at high tide. Only a fraction of the main channel water volume moves onto the marsh surface at stations further downstream, as most of the water movement is up and down the channel of the Duplin. We note however, that NDP and NEP are not biased by the applicability of the night time respiration assumption as both are measured directly as the residual change in DIC or DO during the daytime and 24 h respectively without applying nighttime measures of *R* to estimate daytime gross production.

The metabolism of the Duplin marsh-estuary calculated from inorganic carbon reflected seasonal patterns for GPP, R, and NEP: maximal during warmer months and minimal during the colder months (Fig. 10a). GPP was highest in summer and fall (-0.10 mol m^{-2} d^{-1} to -0.13 mol m^{-2} d^{-1}) and lowest in winter (-0.01 mol m^{-2} d^{-1}) as expected, as

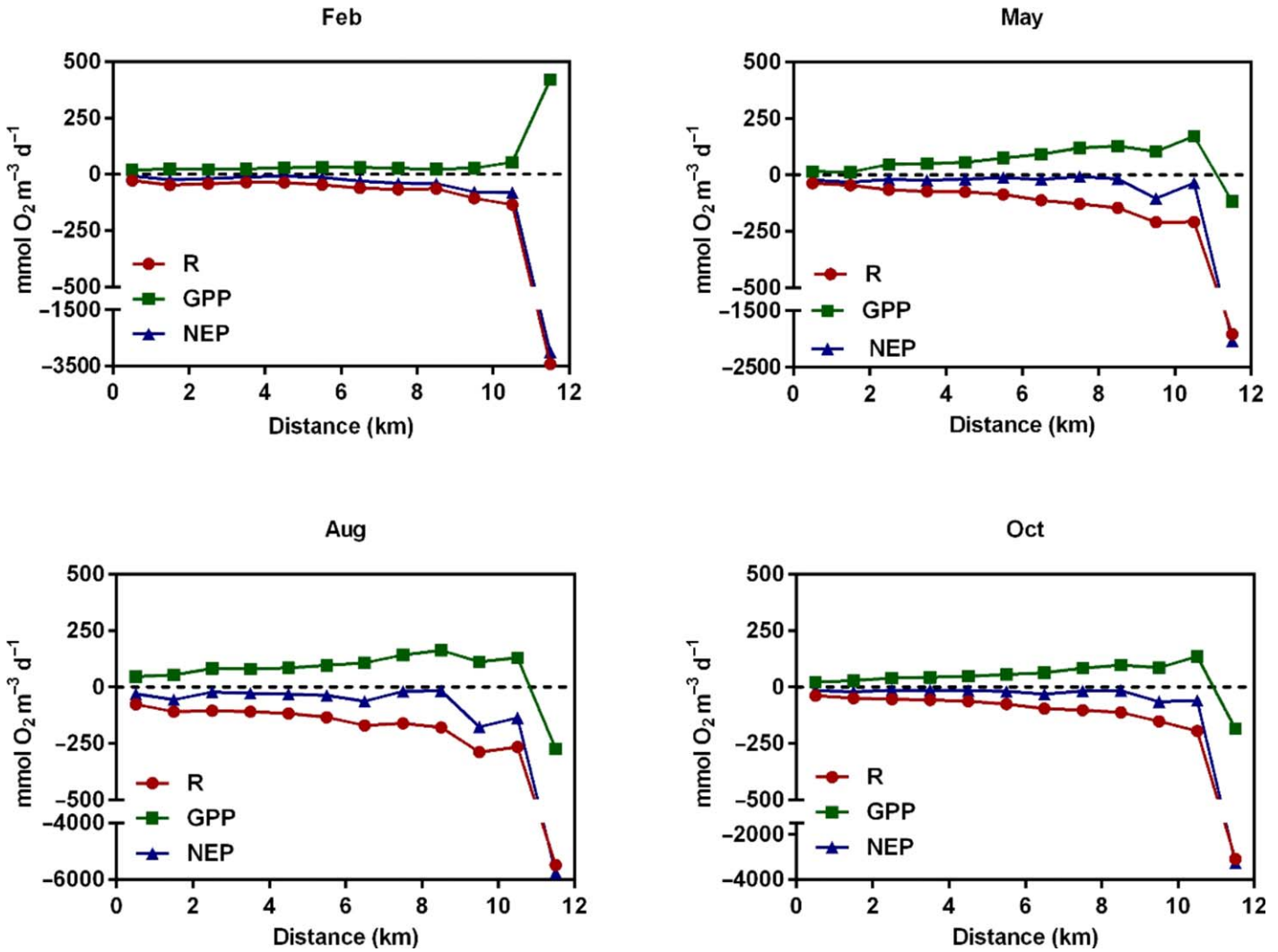

Fig. 9. Distribution of metabolism calculated from changes in DO concentration (labeled O_2) along the Duplin River estuary.

photosynthesis is typically positively related to light intensity and temperature (Darley et al. 1981; Whitney and Darley 1983). GPP was positively related to temperature ($R^2 = 0.58$) and PAR ($R^2 = 0.43$). Respiration peaked in August in response to the higher temperature and DOC availability (Table 1). Regression analysis showed that R is positively related to temperature ($R^2 = 0.86$) and DOC ($R^2 = 0.82$), which is consistent with previous studies showing that respiration rate in marshes and estuaries is regulated by temperature and labile organic carbon availability (Pomeroy et al. 2000). NEP was always net heterotrophic—highest in August (0.06 mol C m^{-2} d^{-1}) and lowest in February (0.02 mol C m^{-2} d^{-1}) (Fig. 10a).

The seasonal pattern of metabolism calculated from DO was typically inverse that calculated by inorganic carbon and showed similar spatial and temporal trends, albeit at lower rates (Fig. 10b). The metabolic rates were usually 30–50% lower calculated by DO than by inorganic C, except for February, when rates based on DO were almost three times higher. This could partially be due to our underestimation of the air–water gas exchange coefficient when intertidal marshes are flooded. This would affect O_2 measures of metabolism more than inorganic C measures as the O_2 inventory in water is more sensitive to gas exchange than that of DIC, which is more sensitive to lateral transport (Cai et al. 1999). However, we suspect the primary reason of a lower O_2-measured metabolic rate is that DO underestimates anaerobic respiration in the short term and completely misses anoxygenic photosynthesis. Anoxygenic photosynthesis has the potential to be substantial in salt marsh systems where S and Fe redox gradients are great in near surface sediments and there is ample light availability.

For estuarine systems where NH_3 is the dominant nutrient taken up in primary production and recycled during decomposition, the stoichiometry of aerobic respiration is 106 moles of O_2 consumed and 106 moles of CO_2 produced

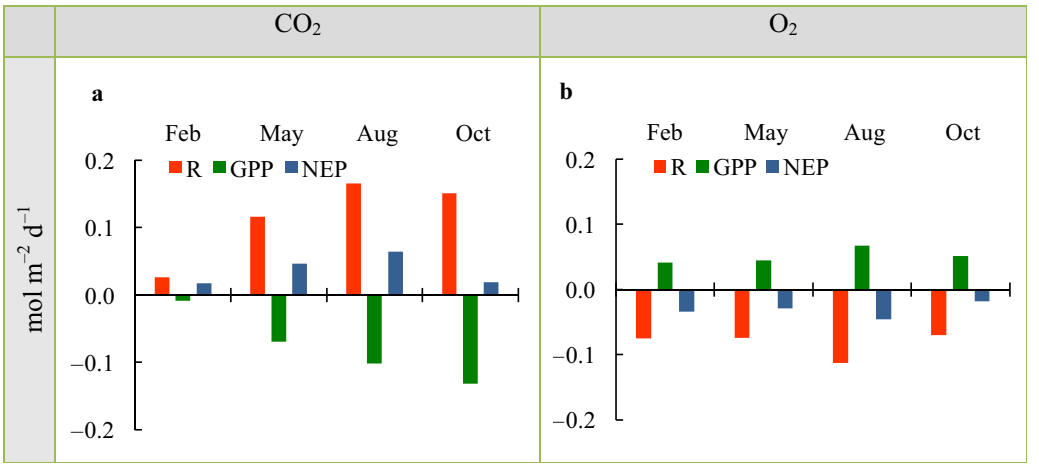

Fig. 10. Seasonal metabolism for the entire Duplin River marsh-estuary as calculated from changes in inorganic carbon (a) and DO (b) (labeled CO_2 and O_2).

(Richards 1965). This differs from the open ocean Redfield stoichiometry of 138 O_2 : 106 CO_2, where primary production is based on HNO_3 uptake. The aerobic estuarine respiration quotient (RQ = CO_2 : O_2) is thus 1.0. In salt marsh and estuarine sediments however, anaerobic respiration raises the RQ as the process does not require O_2 as the terminal electron acceptor yet still releases CO_2. However, anaerobic respiration usually generates reduced metabolic end products (e.g., HS^-) that are ultimately reoxidized (thus consuming O_2). Thus, the deviation of RQ from 1 is dependent on the magnitude of anaerobic respiration and the fate of metabolic end-products.

The mean RQ estimated in this study was 1.2 (1.2 mol CO_2 produced per 1 mol O_2 consumed) but in the metabolically most active seasons (spring, summer and fall) it ranged up to 1.5 (Fig. 11). This is not surprising as salt marsh and estuarine sediments are typically anaerobic within millimeters of the surface (Wiebe et al.1981) with respiration dominated by sulfate reduction (Howarth and Giblin 1983) and the rapid seasonal storage of reduced sulfur and pyrite. In winter however, the RQ was as low as 0.5 indicating less CO_2 production than O_2 consumption. While both aerobic and anaerobic respiration undoubtedly both decreased during the cold season, enhanced O_2 consumption most likely reflects the reoxidation of end-products of summertime anaerobic metabolism.

Due to the technical difficulty of inorganic C-based measures of metabolism, most previous estuarine metabolism and carbon budget studies were achieved by converting O_2-based measures to C units assuming an RQ of 1 (Boynton and Kemp 1985; Hopkinson 1987; Banta et al. 1995). In the few coastal studies where O_2 and inorganic C were both measured, RQ was often reported greater than 1. For example, Dollar et al. (1991) found a RQ of 1.3 by comparing the DIC and O_2 fluxes in Tomales Bay. In Boston Harbor

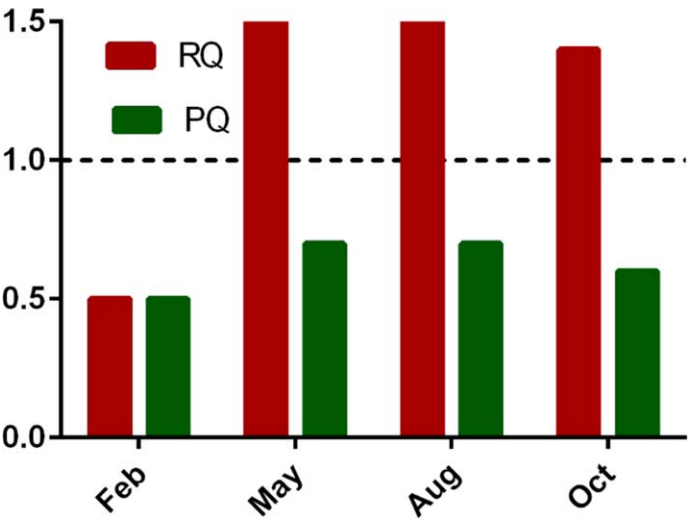

Fig. 11. Seasonality of the RQ and PQ for the entire Duplin River marsh-estuary system. Y-axis is either the ratio of CO_2 : O_2 (RQ) or O_2 : CO_2 (PQ).

sediments, RQs ranged from 1.2 to 2.0 as DIC fluxes were greater than O_2 uptake at two stations in all three study years (Giblin et al.1997). Hopkinson et al (2001) also reported that rates of O_2 consumption were nearly always lower than the release of DIC from sediments of Massachusetts Bay. However, Jiang et al. (2010) found an RQ of nearly 1 in a dark bottle incubation study in continental shelf waters offshore Georgia. With an increasing concern of climate change due to rising atmospheric CO_2 levels from fossil fuel combustion, there is great interest in evaluating the role of the coastal ocean in the global C balance. Our study and others suggest we should be cautious in converting previous metabolic studies from O_2 to CO_2 units and that an RQ of 1 will likely underestimate actual CO_2 production rates.

Table 3. Comparison of aquatic salt marsh-estuarine metabolic rates between this study and the literature. Rates scaled up to the whole system were calculated from previous studies by multiplying their annual areal rates by the relative areas measured in this study.

Process—region or community	Annual total 10^6 mol yr^{-1}	Areal rates mol m^{-2} yr^{-1}	Area estimated in this study 10^6 m^2	Reference
GPP—Duplin salt marsh-estuary	116–CO_2 75–O_2	28–CO_2 18–O_2	Marsh + estuary area: 4.1	This study: open water
GPP-phytoplankton	41	21	Aquatic area ($\leq$ 0 m MSL): 2.0	Ragotzkie (1959): bottles, light-dark O_2
GPP-intertidal benthic algae	25	8	Marsh platform plus creek bank area: 3.1	Pomeroy (1959): Chamber low tide with O_2 High tide with CO_2 Whitney and Darley (1983) (^{14}C)
***R*—Duplin salt marsh-estuary**	176–CO_2 124–O_2	43–CO_2 30–O_2	Marsh + estuary area: 4.1	This study: open water
R-intertidal benthos	71	23	Marsh platform plus creek bank area: 3.1	Pomeroy et al. (1972): chamber with O_2
R-Plankton	44	22	Aquatic area ($\leq$ 0 m MSL): 2.0	Ragotzkie (1959): bottles with O_2
R-Total aquatic respiration of Duplin estuary	116	28	Marsh + estuary area: 4.1	Christian et al. (1981): sum of multiple components
R-plankton (mouth only)	45	23	Estuary area ($\leq$ 0 m MSL): 2.0	Wang and Cai (2004): bottles with CO_2
NEP—Duplin salt marsh-estuary	60–CO_2 49–O_2	14–CO_2 12–O_2	Marsh + estuary area: 4.1	This study

The PQ indicates the balance of O_2 production and the CO_2 consumption through photosynthesis and at Redfield stoichiometry using NH_3 should be 1 (Richards 1965). The calculated PQ for the Duplin system ranged from 0.5 to 0.7 through the year (Fig. 11). This result was not expected but not unreasonable given the light environment and extreme redox gradients near the sediment surface in intertidal mudflats and on the marsh surface. These are ideal conditions for anoxygenic photosynthesis. A variety of bacteria can perform anoxygenic photosynthesis to fix CO_2 to biomass without producing O_2. They use reverse electron transport from electron donors such as sulfide (Cohen et al 1975; Kuenen 1975; Tuttle and Jannasch 1977) or ferrous iron (Widdel et al 1993; Lliros et al 2015), which are abundant in the salt marsh sediment due to anaerobic respiration, to reduce nicotinamide adenine dinucleotide phosphate (NADP+ to NADPH). Kearns et al. (2016) showed that purple sulfur bacteria (Chromatiales) were the 3rd most abundant group of bacteria in salt marshes in the Plum Island Sound estuary. Green sulfur bacteria as well as purple non-sulfur bacteria were common as well. All these groups can express non-oxygenic photosynthesis.

The CO_2–O_2 stoichiometry reported here does not capture the overall stoichiometry of marsh and aquatic landscapes during both flooded and non-flooded conditions. While we are capturing up to 100% of inorganic C and O_2 dynamics during completely flooded conditions (excluding *S. alterniflora* which seems to exchange exclusively with the atmosphere), at low tide in excess of 80% of the total estuarine system is missed by studying water only. The ongoing flux tower study will soon provide nearly continuous data on CO_2 exchange with the atmosphere of the marsh (< 2% tidal creek), and aquatic system when it floods the marsh. It is our future intent to integrate our results with the flux tower CO_2 results to develop an integrated picture for inorganic C. Unfortunately, similar O_2 measures are not a component of flux tower work, so whole system stoichiometry will be impossible to determine until others further examine O_2 dynamics.

We find discrepancies between our results and previous studies in the Duplin River estuary and marshes that differ for GPP and *R* and for O_2 vs. inorganic C approaches. To make comparison, we scaled up previous component measurements, which were usually reported as g C m^{-2} d^{-1}, to moles C yr^{-1} for the entire Duplin salt marsh-estuary using areas we measured in this study. To scale previous measurements of intertidal benthic metabolism on the marsh, we multiplied daily rates by a half year to account for water levels being > 0 MSL only half the time.

For the entire Duplin salt marsh-estuary system, we calculated GPP of 116 $\times$ 10^6 mol C yr^{-1} and 75 $\times$ 10^6 mol O_2 yr^{-1} (Table 3). Ragotzkie measured annual phytoplankton gross production of 41 $\times$ 10^6 mol C yr^{-1} from the light-dark bottle with a PQ of 1.25 (Ragotzkie 1959), which is about a third of our total GPP measured with inorganic C and about

half of our total GPP measured with O_2. Benthic algae contributed 25×10^6 mol C yr^{-1} of GPP with O_2 measured in chambers at high tide and CO_2 measures at low tide with a PQ of 1 (Pomeroy 1959). A similar annual areal production rate was reported by Whitney and Darley (1983), who measured production in bottles using the $^{14}CO_2$ tracer addition approach. Pomeroy's and Whitney's estimates of benthic algal production accounted for about 22% of our total GPP measured with inorganic C and 33% of total GPP with O_2. The sum of the two components (66×10^6 mol yr^{-1} including phytoplankton and intertidal benthic algae) is about 57% of our estimate of total GPP using inorganic C and 80% of our total GPP using O_2. To some extent, this discrepancy reflects the inconsistent PQ conversion factors used in each study (Ragotzkie used 1.25 while Pomeroy used 1) and different measuring techniques (O_2/DIC light-dark, isotopic uptake (^{14}C), bottles and chambers).

We estimate total aquatic respiration of the Duplin salt marsh-estuary to be 176×10^6 mol C yr^{-1} and 124×10^6 mol O_2 yr^{-1}. As expected respiration rates of the various components of the entire system are less than the rates we measured: submerged sediment respiration of 71×10^6 mol C yr^{-1} (Pomeroy et al. 1972) and planktonic respiration of 44×10^6 mol C yr^{-1} (Ragotzkie 1959; Wang and Cai 2004). Christian et al. (1981) estimated total aquatic respiration for the Duplin by integrating rates determined with a combination of various techniques and relative areas of marsh (79%) and open water (21%). We extrapolated his areal rate of R to 116×10^6 mol C yr^{-1} with areas measured in this study. This is very similar to the sum of the components of Pomeroy, Ragotzkie and Wang and Cai (115×10^6 mol C yr^{-1}). Our measurements of respiration are substantially higher than the sum of the component measurements, as we found for GPP: using O_2 our estimate is 7% higher and using inorganic C our estimate is 51% higher. We assume the differences reflect biases in bottle and chamber approaches and arbitrary selection of RQ conversion factors.

It has frequently been observed that rates of metabolism measured in bottles and chambers are consistently less than whole-system measurements. We agree with many previous studies that open water measurements of metabolism are higher than those based on bottle and chamber approaches (Boynton and Kemp 1985; Balsis et al. 1995; Hopkinson and Smith 2005; Cox et al. 2015). Some reasons contributing to these differences include the artifacts associated with containers—reduced turbulence, reduced grazing, unvarying light fields, removal of nutrient supplies from adjacent systems (e.g., benthic recycling for plankton uptake) (Cox et al. 2015), and the lack of system dynamics such as tidal interaction and mixing in component measurements.

Overall, we calculate the Duplin River salt marsh-estuary to be net heterotrophic with R exceeding GPP by 60×10^6 mol C yr^{-1} and 49×10^6 mol O_2 yr^{-1} (Table 3). The O_2-based measure of NEP is the same as the sum of component measures of GPP and R 49×10^6 mol C yr^{-1}. Wang and Cai (2004) estimated Duplin River net heterotrophy at 30×10^6 mol C yr^{-1}. They likely underestimated air–water exchange as they neglected exchange from the flooded marsh and overestimated mixing because they based their DIC gradient on upper estuary vs. oceanic water masses. Component measures of GPP, R, and NEP are consistently in better agreement with our measures based on O_2 than they are with inorganic C. But this agreement is dependent on previous researchers using too low an RQ and too high a PQ, compared to what we actually measured them to be in the Duplin system.

There are few measurements of NEP for other marsh-dominated estuaries. In the York River in Virginia, U.S.A., NEP was estimated to be 8.2 mol C m^{-2} yr^{-1}. This is substantially lower than our Duplin rates (14 mol C m^{-2} yr^{-1} and 12 mol O_2 m^{-2} yr^{-1}). Heterotrophy in the Duplin was also substantially higher than that measured (5.5 mol O_2 m^{-2} yr^{-1}) in the climatically-similar, salt marsh-dominated Grand Bay estuary in the northeastern Gulf of Mexico (Caffrey et al. 2014). However, the level of heterotrophy in the Duplin is much lower than the average of 21 marsh-dominated estuarine sites Caffrey (2004) analyzed using the free-water O_2 technique (approximately 30 mol O_2 m^{-2} yr^{-1}). This is surprising since export of organic material from tidal wetlands is often the most important driver of estuarine heterotrophy, yet the marsh productivity and marsh : water area ratio is nowhere higher than in Georgia.

Uncertainties associated with metabolism estimation

There are two parameters used in calculating air–water gas exchange and dissolved constituent mixing for which there is a considerable uncertainty expressed in the literature: the gas transfer velocity, K_T, and the longitudinal mixing coefficient, ε. To assess the impact of uncertainty in calculations of metabolism, we varied both parameters by what we consider reasonable upper and lower bounds. We varied K_T by a factor of 2 and ε by a factor of 10.

Taking August for example, a tenfold increase in ε increased R-35%, GPP-15%, and NEP-66%. A tenfold reduction decreased R-3%, GPP-0%, and NEP-7%. Multiplying K_T by a factor of 2 gave a 5% increase of GPP, 38% increase of R, and 91% increase of NEP. Dividing K_T by a factor of 2 reduced R 19%, GPP 2%, and NEP 45%. These results show the importance of correctly choosing both these terms, especially for estimates of respiration and NEP. We have confidence in the mixing coefficient for the upper Duplin as it was previously measured empirically by Imberger et al. (1983), but we base our estimate on how the mixing coefficient increases downstream from another system. Our sensitivity analysis shows that increases in the gas transfer velocity impacts estimates of metabolism the most. The factor of 2 range in K_T likely overestimates our uncertainty as the empirical "scatter" in K_T vs. wind speed reported in

Wanninkhof et al. (2009) is only 0.5–1.2 × the rate we chose. If we assume that the marsh canopy does not influence wind speed at the air–water interface and use the Wanninkhof relation to calculate K_T, our annual total system estimates of metabolism change little—9% increase of *R*, 1% increase in GPP, and 21% increase in NEP (data not shown). However, we again note that NEP is more affected than GPP or *R*. As it is the difference in GPP and *R* that is critical in assessing allochthonous organic carbon inputs to the aquatic system and ultimately export to adjacent systems, it is important that we increase our understanding of these critical parameters.

Contribution of the inundated marsh to the Duplin salt marsh-estuary

It is challenging to evaluate the relative importance of the marsh community to overall estuarine aquatic metabolism. Prior attempts have focused on direct quantification of marsh creek bank drainage (Gardner and Gaines 2008) or on quantifying DIC export to the ocean from headwater portions of the Duplin River estuary where the relative area of flooded marsh to open water is very large (e.g., Imberger et al 1983; Wang and Cai 2004). Another approach, which we take in this study, is to consider the mass balances of DIC and DO inputs and outputs over an entire tidal cycle for a very small tidal creek that floods a large marsh platform area. The change in DIC or O_2 after correcting for air–water exchange, is a measure of marsh metabolism in estuarine waters. When scaled to the entire Duplin system, we can assess the relative importance of the marsh compared to the whole salt marsh estuary.

The DIC and O_2 contents of the Duplin River water change when spread out across the tidal creek and its marsh platform or creekshed (Fig. 5) as a result of air–water exchange that is enhanced as the floodwater spreads out across the broad area of the marsh platform and as a result of the metabolism of creek and marsh platform organisms. We estimated the net DIC and DO exchange based on time-course measures of DIC, DO, and pCO_2 calculated from alkalinity and water volume transport calculated from measures of water level height using ArcMap. Even though the Duplin DEM was corrected for a vegetation bias on bare earth elevations, we consider the ArcMap-calculated transport to be a conservative estimate, as the DEM correction may be biased upward slightly because of the extremely dense and tall *S. alterniflora* in the creek channel we studied.

The net lateral transport of DIC between marsh and estuary showed large variation in magnitude and direction for our trips (Fig. 12a). DIC was exported from the creekshed for four out of five sampling months (February, March, May, and August), ranging from 81 mol tide^{-1} to 406 mol tide^{-1} (Fig. 12a). The total lateral transport of O_2 was to the creekshed in May (42 mol tide^{-1}) and from the creekshed to the Duplin in August and October (−69 mol O_2 tide^{-1} and −401 mol O_2 tide^{-1}) (Fig. 12b). While the magnitude and direction were as expected in October based on the DIC transport, the magnitude was lower than expected in May and August and in the opposite direction to DIC in August. No data were collected in February and March for DO.

We calculated a loss of CO_2 to the atmosphere from the tidal creekshed year-round as supersaturated Duplin River water flooded the small tidal creek and spread out across the marsh platform (Fig. 12a). As expected, the O_2 atmospheric exchange was in the opposite direction of CO_2 year-round due to it being under-saturated when entering (Fig. 12b). For CO_2, the air–water loss from the creek ranged from −40 mol tide^{-1} to −577 mol tide^{-1}: lowest in February and highest in magnitude in August. For O_2, the creek gained 237–529 mol tide^{-1} over three seasons. Seasonal variations reflect not only variations in metabolism of the marsh-dominated tidal creek but also variations in extent of marsh and marsh organisms flooded.

Areal rates of lateral transport from the marsh and tidal creek to the Duplin River ranged from 5 mmol DIC m^{-2} tide^{-1} to 31 mmol DIC m^{-2} tide^{-1} for four of five observation periods (Fig. 12c). The average magnitude of this flux is very similar to the reduction in marsh-air flux as measured with the eddy covariance approach when the marsh floods (Kathilankal et al. 2008): 23 mmol C m^{-2} d^{-1} DIC export (taking into account two tides per day) vs. 19 ± 2 mmol C m^{-2} d^{-1} NEE reduction in a Virginia salt marsh. The areal transport of O_2 from the tidal creek was to the creekshed from the Duplin in May (4 mmol m^{-2} tide^{-1}) and from the creekshed to the Duplin in August and October (−3 mmol O_2 m^{-2} tide^{-1} to −19 mmol O_2 m^{-2} tide^{-1}) (Fig. 12d).

Flux tower measurements of salt marsh NEE miss any measure of marsh metabolism into floodwater at high tide and exported during ebb tide. Indeed, tidal marsh flux tower studies show a sizeable reduction in NEE fluxes when the marsh is inundated (e.g., *see* Forbrich and Giblin 2015). To estimate true marsh NEP, flux tower NEE measures must be corrected for lateral exchange as measured in our study.

The metabolism of the tidal creek—marsh platform system, estimated from balancing lateral transport and air–water exchange, revealed a strong seasonal pattern of being heterotrophic for most of the year (negative NDP meaning *R* exceeding GPP in February, March, May, and August, ranging from 31 mmol C m^{-2} tide^{-1} to 49 mmol C m^{-2} tide^{-1}) and autotrophic in October (positive NDP meaning GPP exceeding *R* by 7 mmol C m^{-2} tide^{-1}) (Fig. 12c). In October, the net consumption of DIC (generation of DO) occurred during a cloudless day when cumulative PAR was 28% higher than typical for this time of year and when high tide coincided with peak solar radiation. The net uptake of DIC suggests an autotrophic marsh platform during the hours the marsh was flooded in October. It would appear that for most of the year the marsh-creek system is heterotrophic ($R > GPP$) even during the daytime. Only when

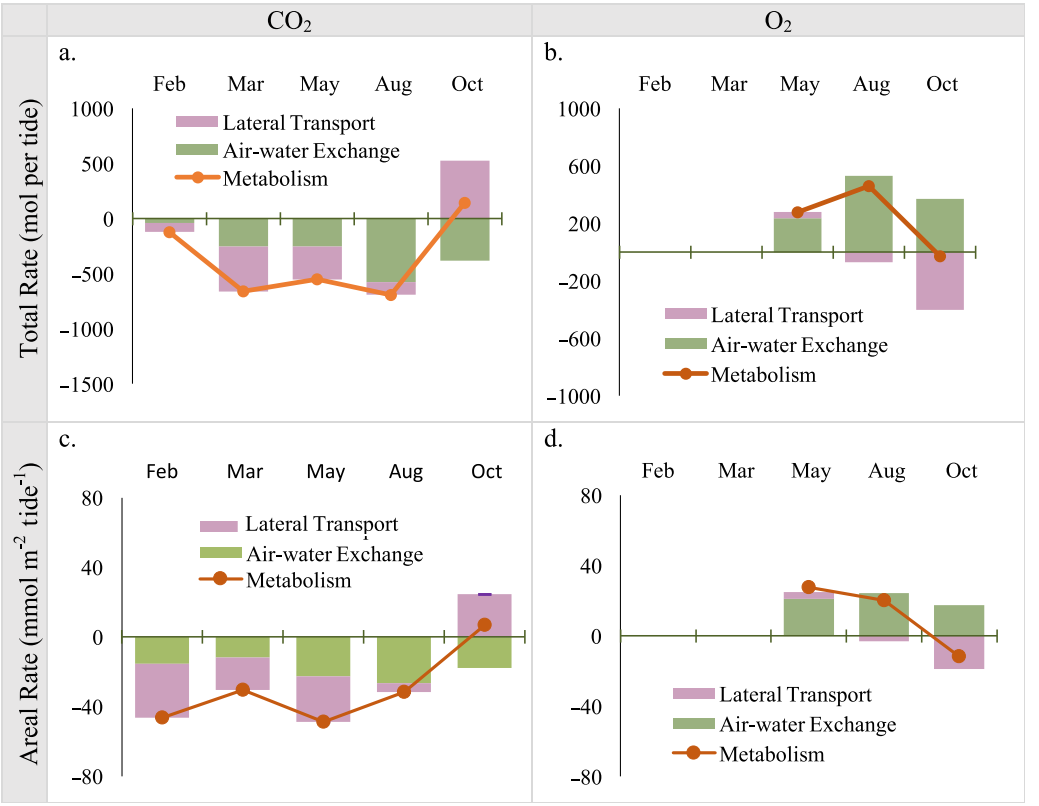

Fig. 12. Air–water exchange, lateral transport and metabolism of the inundated marsh calculated from inorganic carbon and DO approaches (labeled as CO_2 and O_2). (a) and (b): total rates calculated with C and O_2 respectively. (c) and (d): areal rates calculated with C and O_2 respectively. Negative transport indicates loss from the marsh to the estuary or the atmosphere and vice versa for positive transport. Areal rates were calculated by dividing the total rates with ½ the maximum area of marsh flooded each month: 2600 m^2, 21,500 m^2, 11,000 m^2, 21,800 m^2, and 21,500 m^2 for February, March, May, August, and October, respectively. We did not collect O_2 data in February and March. Net daytime production on the marsh (NDP) was calculated as the sum of the vertical flux and the average lateral transport.

photosynthetic conditions are ideal such as we found in October (highest daily PAR of entire study and perfectly matched with time of high tide) is the marsh-creek system autotrophic.

Measurements in the winter (February and March) give us some insight into the relative influence of the marsh platform vs. the vegetated intertidal creekbank on DIC dynamics. In February, only the intertidal marsh creekbank was flooded (0.84 m MSL high tide), while in March both creekbank and platform marshes were flooded (1.34 m MSL high tide). We assume little change in metabolism between these 2 months as weather conditions were similar. Net DIC export was 81 mol $tide^{-1}$ in February and 406 mol $tide^{-1}$ in March. Thus, the marsh platform contributes 80% ((406–81)/406) compared to 20% for the marsh creekbank. Taking into consideration the total tidal creek shoreline length 862 m (both sides of creek), the creek bank exported 0.094 mol DIC m^{-1} shoreline and the marsh platform exported 0.019 mol DIC m^{-2} (based on 43,000 m^2 more of marsh flooded). We expect that a major source of this DIC is microbial respiration in creekbank sediments, which drain at low tide (this drainage is sometimes described as a component of submarine groundwater discharge). The advective movement of water into and out of creekbank sediments amplifies the export of respiratory DIC produced there, making this a hotspot of activity within meso- and macrotidal estuaries. A meter of marsh edge contributes about five times more DIC to the overall Duplin saltmarsh estuary, than a m^2 of marsh platform. If salt marshes do not keep up with sea-level rise and they begin to fragment as described by Reed (2002) and Hopkinson and Day (1977), we can expect tidal creek density to increase while total marsh area decreases. Our results suggest this pattern will lead to more DIC export to the estuary at least until marsh area loss becomes really large.

As mentioned earlier, for the most part the tidal creek—marsh platform system was heterotrophic, even during daytime hours. Assuming net daytime heterotrophy on the marsh in this study is a minimal estimate of respiration and that the small tidal creek marsh is representative of marshes throughout the entire Duplin, we find that flooding marshes contribute from 12% to 35% of total respiration measured for the entire Duplin (Table 4). We note that this influence reflects the marsh only being flooded for 3–4.2 h out of the total 12-h day/night interval.

Table 4. Comparisons between marsh NDP and the total system respiration (*R*).

	May	Aug		Oct
Marsh NDP (10^5 mol C tide^{-1})	1.2	0.8	Marsh NDP	−0.2
Total daytime *R* (10^5 mol C tide^{-1})	4.7	6.6	Total night *R*	5.1
% Marsh NDP of total daytime *R*	26%	12%	Marsh *R* (assuming 12–36% of total *R*)	0.61–1.8
Total nighttime *R* (10^5 mol C tide^{-1})	3.4	5.3	Marsh GPP (=|NDP−*R*|)	0.81–2.0
% Marsh NDP of total nighttime *R*	35%	15%	% Marsh contributed GPP	10–24%

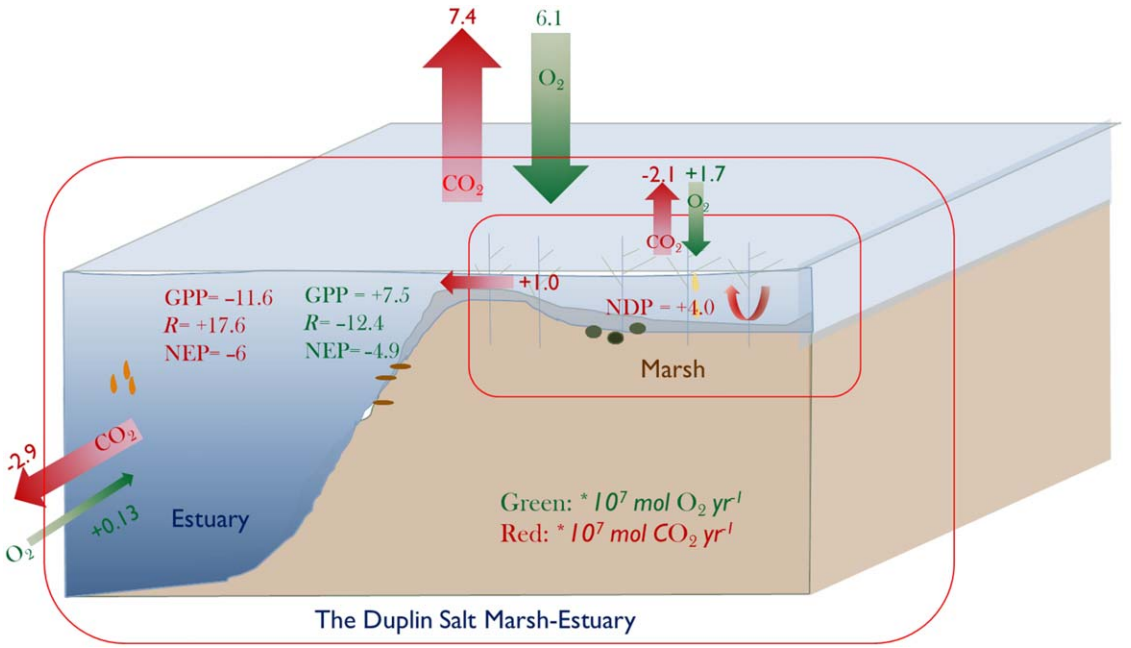

Fig. 13. A conceptual representation of marsh-estuary metabolism and CO_2 and O_2 dynamics for the Duplin River system, highlighting the exchange between the marsh and tidal waters, the exchange between the entire Duplin marsh-estuary and the atmosphere and the coastal ocean. Dissolved inorganic C and oxygen exchanges are labeled CO_2 and O_2. Metabolism (GPP, *R*, NEP, and NDP) calculated from inorganic carbon and DO approaches are shown in red and green color, respectively.

Under the ideal conditions observed in October, the inundated marsh was net autotrophic during the day, which enables us to estimate the extent to which the inundated marsh can contribute to total Duplin system GPP. GPP equals NDP plus night *R*. Tidal creek—marsh platform NDP in October was -0.2×10^6 mol C tide^{-1} (net autotrophic). Estimating *R* on the inundated marsh as 12–35% of measured whole system night respiration in October (from above) and adding to October tidal creek—marsh platform NDP yields an estimate of tidal creek-marsh platform GPP ranging from −0.8 mol C tide^{-1} to -2.0×10^5 mol C tide^{-1}. Scaled to all marshes of the Duplin marsh-estuary, we estimate that the inundated marsh can contribute 10–24% of the total system GPP under ideal conditions.

These estimates of the relative contribution of the inundated marsh to total Duplin aquatic system metabolism are first approximations and presumably conservative. Respiration on the marsh at night is undoubtedly higher than that estimated from the net change in DO or DIC during daytime. Nevertheless, these are the first ever estimates of the extent to which aquatic metabolism as measured by the free-water approach integrates a portion of overall marsh metabolism.

We can conceptualize the marsh community to include emergent macrophytes, here *S. alterniflora*, the micro-, meio-, and macrofauna of the marsh sediments and surface muds, organisms suspended in the floodwaters, and epiphytic algal and bacterial organisms on and in surface sediments and live and dead-standing marsh macrophytes. When flooded, these sub-communities metabolize directly into flood waters, with exception of the marsh macrophytes themselves. It is unclear to what extent, if any, macrophytes exchange CO_2 or oxygen with flood waters as opposed to the atmosphere. With exception of air-

breathing organisms, the vast majority of metabolism will be attributable to bacteria, which when active are primarily moist and thus producing metabolic gases directly into water. As a result, gas exchange is limited and DIC concentrations and oxygen deficits accumulate in sediment pore waters. Koretsky et al. (2000) showed pore-water concentrations of Fe^{2+}, Mn^{2+}, H_2S, and alkalinity to exceed 450 μM, 200 μM, 4000 μM, and 24,000 μM, respectively, in salt-marsh sediments at Sapelo Island, which can result in sediment to floodwater fluxes when the marsh is inundated. These fluxes are the result of prior metabolism and therefore represent more than just the 3–4.2 h during which the marsh platform is inundated.

Conclusion

Metabolism dominated inorganic C and O_2 dynamics within the overall Duplin River salt marsh-estuary and respiration greatly exceeded GPP for both inorganic C and O_2 -based measurements (Fig. 13). Overall system heterotrophy demonstrated a strong dependence on excess primary production by marsh macrophytes as the fuel for this excess respiration. The aquatic system is strongly linked to the adjacent tidal marshes via the twice daily tidal flooding. During flood tides, waters capture a portion of the metabolism occurring on the marsh resulting in a loss of CO_2 to the atmosphere (or gain of O_2) and an export of DIC to the Duplin (or import of O_2). A large percentage of overall air–water exchange of dissolved gases in the estuary occurs from waters when they flood the marsh. We have likely underestimated the air–water flux over the marsh because we have assumed no effect of wind on the exchange rate. This is one of the largest sources of uncertainty in our analysis. The Duplin estuary is also a source of DIC to the coastal ocean (and sink for O_2), but at a reduced magnitude relative to the air–water flux. We found that the $CO_2:O_2$ stoichiometry of metabolism deviates substantially from oceanographic Redfield ratios with an average RQ of 1.2 and PQ of 0.6. We attribute the high RQ to the importance of sulfate reduction and the burial of pyrite in salt marsh sediments. We attribute the low PQ to the importance of anoxygenic photosynthesis. We suggest that future work in developing C budgets for coastal ecosystems be careful in choosing factors to convert from O_2 to CO_2 units. It is our hope that this paper stimulates discussion and further research into gas exchange from tidally flooded wetlands in estuarine systems, the magnitude and controls of anoxygenic photosynthesis in tidal salt marshes, and the overall C and O_2 budgets and linkage of marsh and aquatic subsystems of marsh-dominated estuaries.

References

Balsis, B. R., D. W. Alderman, I. D. Buffam, R. H. Garritt, C. S. Hopkinson, and J. J. Vallino. 1995. Total system metabolism of the Plum Island Sound estuarine system. Biol. Bull. **189**: 252–254. doi:10.1086/BBLv189n2p252

Banta, G. T., A. E. Giblin, J. E. Hobbie, and J. Tucker. 1995. Benthic respiration and nitrogen release in Buzzards Bay, Massachusetts. J. Mar. Res. **53**: 107–135. doi:10.1357/0022240953213287

Bauer, J. E., W. J. Cai, P. A. Raymond, T. S. Bianchi, C. S. Hopkinson, and P. A. Regnier. 2013. The changing carbon cycle of the coastal ocean. Nature **504**: 61–70. doi:10.1038/nature12857

Boynton, W. R., and W. M. Kemp. 1985. Nutrient regeneration and oxygen consumption by sediments along an estuarine salinity gradient. Mar. Ecol. Prog. Ser. **23**: 45–55. doi:10.3354/meps023045

Caffrey, J. M. 2004. Factors controlling net ecosystem metabolism in US estuaries. Estuaries **27**: 90–101. doi:10.1007/BF02803563

Caffrey, J. M., M. C. Murrell, K. S. Amacker, J. W. Harper, S. Phipps, and M. S. Woodrey. 2014. Seasonal and interannual patterns in primary production, respiration, and net ecosystem metabolism in three estuaries in the northeast Gulf of Mexico. Estuaries Coast. **37**: 222–241. doi:10.1007/s12237-013-9701-5

Cai, W. J. 2011. Estuarine and coastal ocean carbon paradox: CO_2 sinks or sites of terrestrial carbon incineration? Ann. Rev. Mar. Sci. **3**: 123–145. doi:10.1146/annurev-marine-120709-142723

Cai, W. J., and Y. Wang. 1998. The chemistry, fluxes, and sources of carbon dioxide in the estuarine waters of the Satilla and Altamaha Rivers, Georgia. Limnol. Oceanogr. **43**: 657–668. doi:10.4319/lo.1998.43.4.0657

Cai, W. J., L. R. Pomeroy, M. A. Moran, and Y. Wang. 1999. Oxygen and carbon dioxide mass balance for the estuarine-intertidal marsh complex of five rivers in the southeastern US. Limnol. Oceanogr. **44**: 639–649. doi:10.4319/lo.1999.44.3.0639

Carini, S., N. Weston, C. Hopkinson, J. Tucker, A. Giblin, and J. Vallino. 1996. Gas exchange rates in the Parker River estuary, Massachusetts. The Biological Bulletin, **191**: 333–334.

Christian, R. R., R. B. Hanson, J. R. Hall, and W. J. Wiebe. 1981. Aerobic microbes and meiofauna, p. 113–135. In L. R. Pomeroy, R. G. Wiegert [eds.], The ecology of a salt marsh. Springer.

Cohen, Y., E. Padan, and M. Shilo. 1975. Facultative anoxygenic photosynthesis in the cyanobacterium Oscillatoria limnetica. J. Bacteriol. **123**: 855–861.

Cox, T. J., T. Maris, K. Soetaert, J. C. Kromkamp, P. Meire, and F. Meysman. 2015. Estimating primary production from oxygen time series: A novel approach in the frequency domain. Limnol. Oceanogr.: Methods **13**: 529–552. doi:10.1002/lom3.10046

Darley, W. M., C. L. Montague, F. G. Plumley, W. W. Sage, and A. T. Psalidas. 1981. Factors limiting edaphic algal

biomass and productivity in a Georgia salt marsh. Journal of Phycology **17**: 122–128.

Darnell, R. M. 1967. Organic detritus in relation to the estuarine ecosystem. Estuaries **83**: 376–382.

Dollar, S. J., S. V. Smith, S. M. Vink, S. Obrebski, and J. T. Hollibaugh. 1991. Annual cycle of benthic nutrient fluxes in Tomales Bay, California, and contribution of the benthos to total ecosystem metabolism. Mar. Ecol. Prog. Ser. **79**: 115–125. doi:10.3354/meps079115

Faber, P. A., V. Evrard, R. J. Woodland, I. C. Cartwright, and P. L. Cook. 2014. Pore-water exchange driven by tidal pumping causes alkalinity export in two intertidal inlets. Limnol. Oceanogr. **59**: 1749–1763. doi:10.4319/lo.2014.59.5.1749

Fairaill, C. W., J. E. Hare, J. B. Edson, and W. McGillis. 2000. Parameterization and micrometeorological measurement of air–sea gas transfer. Boundary Layer Meteorol. **96**: 63–106. doi:10.1023/A:1002662826020

Forbrich, I., and A. E. Giblin. 2015. Marsh-atmosphere CO_2 exchange in a New England salt marsh. J. Geophys. Res. Biogeosci. **120**: 1825–1838. doi:10.1002/2015JG003044

Frankignoulle, M., G. Abril, A. Borges, I. Bourge, C. Canon, B. Delille, E. Libert, and J. M. Théate. 1998. Carbon dioxide emission from European estuaries. Science **282**: 434–436. doi:10.1126/science.282.5388.434

Frey, R. W., and P. B. Basan. 1978. Coastal salt marshes, p. 101–169. *In* A. Richard, Jr. Davis [eds], Coastal sedimentary environments. Springer.

Gardner, L. R., and E. F. Gaines. 2008. A method for estimating pore water drainage from marsh soils using rainfall and well records. Estuar. Coast. Shelf Sci. **79**: 51–58. doi:10.1016/j.ecss.2008.03.014

Giblin, A. E., C. S. Hopkinson, and J. Tucker. 1997. Benthic metabolism and nutrient cycling in Boston Harbor, Massachusetts. Estuaries **20**: 346–364. doi:10.2307/1352349

Hansen, D. V., and M. Rattray. 1966. New dimensions in estuary classification. Limnol. Oceanogr. **11**: 319–326. doi:10.4319/lo.1966.11.3.0319

Hladik, C., and M. Alber. 2012. Accuracy assessment and correction of a LIDAR-derived salt marsh digital elevation model. Remote Sens. Environ. **121**: 224–235. doi:10.1016/j.rse.2012.01.018

Ho, D. T., C. J. Zappa, W. R. McGillis, L. F. Bliven, B. Ward, J. W. Dacey, P. Schlosser, and M. B. Hendricks. 2004. Influence of rain on air-sea gas exchange: Lessons from a model ocean. J. Geophys. Res. Oceans **109**. doi:10.1029/2003JC001806

Hopkinson, Jr., C. S. 1985. Shallow-water benthic and pelagic metabolism. Mar. Biol. **87**: 19–32. doi:10.1007/BF00397002

Hopkinson, Jr., C. S. 1987. Nutrient regeneration in shallow-water sediments of the estuarine plume region of the nearshore Georgia Bight, USA. Mar. Biol. **94**: 127–142. doi:10.1007/BF00392905

Hopkinson, Jr., C. S. 1988. Patterns of organic carbon exchange between coastal ecosystems, p. 122–154. *In* J. Bengt-Owe [ed.], Coastal-offshore ecosystem interactions. Springer.

Hopkinson, C. S., and J. W. Day, Jr. 1977. A model of the Barataria Bay salt marsh ecosystem, p. 236–265. *In* A. S. H. Charles, J. W. Day [eds], Ecosystem modeling in theory and practice. Wiley-Interscience.

Hopkinson, Jr., C. S., A. E. Giblin, and J. Tucker. 2001. Benthic metabolism and nutrient regeneration on the continental shelf of Eastern Massachusetts, USA. Mar. Ecol. Prog. Ser. **224**: 1–19. doi:10.3354/meps224001

Hopkinson, C. S., and E. M. Smith. 2005. Estuarine respiration: An overview of benthic, pelagic, and whole system respiration. Respir. Aquat. Ecosyst. 122–146. doi:10.1093/acprof:oso/9780198527084.003.0008

Howarth, R. W., and A. Giblin. 1983. Sulfate reduction in the salt marshes at Sapelo Island, Georgia. Limnol. Oceanogr. **28**: 70–82. doi:10.4319/lo.1983.28.1.0070

Imberger, J., T. Bermun, R. R. Christian, and W. J. Wiebe. 1983. The influence of water motion on the distribution and transport of materials in a salt marsh estuary. Limnol. Oceanogr. **28**: 201–214. doi:10.4319/lo.1983.28.2.0201

Jiang, L. Q., W. J. Cai, Y. Wang, J. Diaz, P. L. Yager, and X. Hu. 2010. Pelagic community respiration on the continental shelf off Georgia, USA. Biogeochemistry **98**: 101–113. doi:10.1007/s10533-009-9379-8

Kathilankal, J. C., T. J. Mozdzer, J. D. Fuentes, P. D'Odorico, K. J. McGlathery, and J. C. Zieman. 2008. Tidal influences on carbon assimilation by a salt marsh. Environ. Res. Lett. **3**: 044010. doi:10.1088/1748-9326/3/4/044010

Kearns, P. J., J. H. Angell, E. M. Howard, L. A. Deegan, R. H. Stanley, and J. L. Bowen. 2016. Nutrient enrichment induces dormancy and decreases diversity of active bacteria in salt marsh sediments. Nat. Commun. **7**: 12881. doi:10.1038/ncomms12881

Koretsky, C., C. Meile, B. Curry, J. Haas, K. Hunter, and K. Van Cappellen. 2000. The effect of colonization by *Spartina alterniflora* on pore water redox geochemistry at a saltmarsh on Sapelo Island, GA. J. Conf. Abstr. **5**: 599.

Koretsky, C. M., C. M. Moore, K. L. Lowe, C. Meile, T. J. DiChristina, and P. Van Cappellen. 2003. Seasonal oscillation of microbial iron and sulfate reduction in saltmarsh sediments (Sapelo Island, GA, USA). Biogeochemistry **64**: 179–203. doi:10.1023/A:1024940132078

Kuenen, J. G. 1975. Colourless sulfur bacteria and their role in the sulfur cycle. Plant Soil **43**: 49–76. doi:10.1007/BF01928476

Lightbody, A. F., and H. M. Nepf. 2006. Prediction of velocity profiles and longitudinal dispersion in salt marsh vegetation. Limnol. Oceanogr. **51**: 218–228. doi:10.4319/lo.2006.51.1.0218

Llirós, M., T. García–Armisen, F. Darchambeau, C. Morana, X. Triadó–Margarit, Ö. Inceoğlu, C. M. Borrego, S. Bouillon, P. Servais, A. V. Borges, J.-P. Descy, D. E. Canfield, and S. A. Crowe. 2015. Pelagic photoferrotrophy and iron cycling in a modern ferruginous basin. Sci. Rep. **5**. doi:10.1038/srep13803

Mcknight, C. J. 2016. A modeling study of horizontal transport and residence time in the Duplin River estuary, Sapelo Island GA. M.S. thesis. Univ. of Georgia.

Montague, C. L. 1980. A natural history of temperate western Atlantic fiddler crabs (genus Uca) with reference to their impact on the salt marsh. Contrib. Mar. Sci. **23**: 25–55.

Neubauer, S. C., and I. C. Anderson. 2003. Transport of dissolved inorganic carbon from a tidal freshwater marsh to the York River estuary. Limnol. Oceanogr. **48**: 299–307. doi:10.4319/lo.2003.48.1.0299

Nixon, S. W. 1980. Between coastal marshes and coastal waters—a review of twenty years of speculation and research on the role of salt marshes in estuarine productivity and water chemistry, p. 437–525. Springer.

Odum, E. P. 1968. Energy flow in ecosystems: A historical review. Am. Zool. **8**: 11–18. doi:10.1093/icb/8.1.11

Odum, H. T. 1956. Primary production in flowing waters. Limnol. Oceanogr. **1**: 102–117. doi:10.4319/lo.1956.1.2.0102

Odum, H. T., and C. M. Hoskin. 1958. Comparative studies on the metabolism of marine waters. Publ. Inst. Mar. Sci Texas **5**: 16–46.

Odum, H. T., and R. F. Wilson. 1962. Further studies on reaeration and metabolism of Texas bays, 1958–1960. Publ. Inst. Mar. Sc., Univ. Tex., **8**: 23–55.

Omstedt, A., C. Humborg, J. Pempkowiak, M. Perttilä, A. Rutgersson, B. Schneider, and B. Smith. 2014. Biogeochemical control of the coupled CO_2–O_2 system of the Baltic Sea: A review of the results of Baltic-C. Ambio **43**: 49–59. doi:10.1007/s13280-013-0485-4

Peterson, B., B. Fry, M. Hullar, S. Saupe, and R. Wright. 1994. The distribution and stable carbon isotopic composition of dissolved organic carbon in estuaries. Estuaries **17**: 111–121. doi:10.2307/1352560

Pomeroy, L. R. 1959. Algal productivity in salt marshes of Georgia. Limnol. Oceanogr. **4**: 386–397. doi:10.4319/lo.1959.4.4.0386

Pomeroy, L. R., L. R. Shenton, R. D. H. Jones, and R. J. Reimold. 1972. Nutrient flux in estuaries, p. 274–279. *In* G. E. Likens [ed.], Nutrients and eutrophication. Spec. Symp. 1.

Pomeroy, L. R., J. E. Sheldon, W. M. Sheldon, J. O. Blanton, J. Amft, and F. Peters. 2000. Seasonal changes in microbial processes in estuarine and continental shelf waters of the south-eastern USA. Estuar. Coast. Shelf Sci. **51**: 415–428. doi:10.1006/ecss.2000.0690

Pomeroy, L. R., and R. G. Wiegert [eds.]. 2012. The ecology of a salt marsh. V. **38**. Springer Science & Business Media.

Ragotzkie, R. A. 1959. Plankton productivity in estuarine waters of Georgia. Publ. Inst. Mar. Sci. Univ. Texas **6**: 146–158.

Ragotzkie, R. A., and R. A. Bryson. 1955. Hydrography of the Duplin River, Sapelo Island, Georgia. Bull. Mar. Sci. **5**: 297–314.

Raymond, P. A., J. E. Bauer, and J. J. Cole. 2000. Atmospheric CO_2 evasion, dissolved inorganic carbon production, and net heterotrophy in the York River estuary. Limnol. Oceanogr. **45**: 1707–1717. doi:10.4319/lo.2000.45.8.1707

Raymond, P.A., and J. J. Cole. 2001. Gas exchange in rivers and estuaries: Choosing a gas transfer velocity. Estuaries and Coasts **24**: 312–317.

Raymond, P. A., and C. S. Hopkinson. 2003. Ecosystem modulation of dissolved carbon age in a temperate marsh-dominated estuary. Ecosystems **6**: 694–705. doi:10.1007/s10021-002-0213-6

Redfield, A. C. 1958. The biological control of chemical factors in the environment. Am. Sci. **46**: 230A–221.

Reed, D. J. 2002. Sea-level rise and coastal marsh sustainability: Geological and ecological factors in the Mississippi delta plain. Geomorphology **48**: 233–243. doi:10.1016/S0169-555X(02)00183-6

Richards, F. A. 1965. Anoxic basins and fjords. Academic Press.

Smith, S. V., and J. T. Hollibaugh. 1997. Annual cycle and interannual variability of ecosystem metabolism in a temperate climate embayment. Ecol. Monogr. **67**: 509–533. doi:10.1890/0012-9615(1997)067[0509:ACAIVO]2.0.CO;2

Sottile II, W. S. 1973. Studies of microbial production and utilization of dissolved organic carbon in a Georgia salt marsh-estuarine ecosystem, p. 153. Ph.D. thesis. Univ. of Georgia.

Swaney, D. P., R. W. Howarth, and T. J. Butler. 1999. A novel approach for estimating ecosystem production and respiration in estuaries: Application to the oligohaline and mesohaline Hudson River. Limnol. Oceanogr. **44**: 1509–1521. doi:10.4319/lo.1999.44.6.1509

Teal, J. M. 1962. Energy flow in the salt marsh ecosystem of Georgia. Ecology **43**: 614–624. doi:10.2307/1933451

Tobias, C. R., J. K. Böhlke, and J. W. Harvey. 2007. The oxygen-18 isotope approach for measuring aquatic metabolism in high productivity waters. Limnol. Oceanogr. **52**: 1439–1453. doi:10.4319/lo.2007.52.4.1439

Tuttle, J. H., and H. W. Jannasch. 1977. Thiosulfate stimulation of microbial dark assimilation of carbon dioxide in shallow marine waters. Microb. Ecol. **4**: 9–25. doi:10.1007/BF02010426

Vallino, J. J., and C. S. Hopkinson, Jr. 1998. Estimation of dispersion and characteristic mixing times in Plum Island Sound estuary. Estuar. Coast. Shelf Sci. **46**: 333–350. doi:10.1006/ecss.1997.0281

Vallino, J. J., C. S. Hopkinson, and R. H. Garritt. 2005. Estimating estuarine gross production, community respiration and net ecosystem production: A nonlinear inverse technique. Ecol. Modell. **187**: 281–296. doi:10.1016/j.ecolmodel.2004.10.018

Wadsworth, J. 1980. Geomorphology and hydrography of the Duplin River estuarine system. Doctoral dissertation, Ph.D. thesis. Univ. of Georgia.

Wang, Z. A., and W. J. Cai. 2004. Carbon dioxide degassing and inorganic carbon export from a marsh-dominated estuary (the Duplin River): A marsh CO_2

pump. Limnol. Oceanogr. **49**: 341–354. doi:10.4319/lo.2004.49.2.0341

Wanninkhof, R., W. E. Asher, D. T. Ho, C. Sweeney, and W. R. McGillis. 2009. Advances in quantifying air-sea gas exchange and environmental forcing. Mar. Sci. **1**: 213–244. doi:10.1146/annurev.marine.010908.163742

Weiss, R. 1974. Carbon dioxide in water and seawater: the solubility of a non-ideal gas. Marine chemistry **2**: 203–215.

Whitney, D. E., and W. M. Darley. 1983. Effect of light intensity upon salt marsh benthic microalgal photosynthesis. Mar. Biol. **75**: 249–252. doi:10.1007/BF00406009

Widdel, F., S. Schnell, S. Heising, A. Ehrenreich, B. Assmus, and B. Schink. 1993. Ferrous iron oxidation by anoxygenic phototrophic bacteria. Nature **362**: 834–836. doi:10.1038/362834a0

Wiebe, W. J., R. R. Christian, J. A. Hansen, G. King, B. Sherr, and G. Skyring. 1981. Anaerobic respiration and fermentation, p. 137–159. *In* L. R. Pomeroy, and R. G. Wiegert [eds.], The ecology of a salt marsh. Springer.

Wiegert, R. G., L. R. Pomeroy, and W. J. Wiebe. 1981. Ecology of salt marshes: an introduction. *In* The ecology of a salt marsh pp. 3–19. Springer New York.

Zappa, C. J., W. R. McGillis, P. A. Raymond, J. B. Edson, E. J. Hintsa, H. J. Zemmelink, J. W. Dacey, and D. T. Ho. 2007. Environmental turbulent mixing controls on air-water gas exchange in marine and aquatic systems. Geophys. Res. Lett. **34**. L10601. doi:10.1029/2006GL028790

Zhai, W. D., M. Dai, and W. J. Cai. 2009. Coupling of surface pCO_2 and dissolved oxygen in the northern South China Sea: Impacts of contrasting coastal processes. Biogeosciences **6**: 2589–2598.

Acknowledgment

We thank Caroline Reddy, Joel Craig, Jacob Shalack, Emily Davenport, Kim Hunter, Baoshan Chen, and Liang Wang for their field and laboratory assistance and companionship. This is also Contribution #1053 by the University of Georgia, Marine Institute on Sapelo Island. Cai also acknowledges the National Aeronautics and Space Administration (NNX14AM37G) for supporting his research. This study was funded by National Science Foundation, GCE-LTER program (NSF-OCE-1237140).

Conflict of Interest

None declared.

Submitted 21 October 2016
Revised 24 April 2017
Accepted 10 May 2017

Associate editor: Jim Falter